Available online at www.sciencedirect.com
ScienceDirect
Geochimica et Cosmochimica Acta 73 (2009) 3423–3449
Geochimica et Cosmochimica Acta
www.elsevier.com/locate/gca

Primitive off-rift basalts from Iceland and Jan Mayen: Os-isotopic evidence for a mantle source containing enriched subcontinental lithosphere

Vinciane Debaille [a,b,*], Reidar G. Trønnes [c,d], Alan D. Brandon [e], Tod E. Waight [f], David W. Graham [g], Cin-Ty A. Lee [h]

[a] *Département des Sciences de la Terre et de l'Environnement, Université Libre de Bruxelles, CP160/02, 50 Av. F.D. Roosevelt, B-1050 Brussels, Belgium*
[b] *Lunar and Planetary Institute, 3600 Bay Area Bld, Houston, TX 77058, USA*
[c] *Nordic Volcanological Center, Institute of Earth Sciences, University of Iceland, Reykjavik, Iceland*
[d] *Natural History Museum, University of Oslo, PO Box 1172, 0318 Oslo, Norway*
[e] *NASA Johnson Space Center, Mail Code KR, Building 31, Houston, TX 77058, USA*
[f] *Institute of Geography and Geology, University of Copenhagen, Øster Voldgade 10, 1350 Copenhagen K, Denmark*
[g] *College of Oceanic and Atmospheric Sciences, Oregon State University, Corvallis, OR 97331, USA*
[h] *Department of Earth Science, MS-126, Rice University, PO Box 1892, Houston, TX 77251-1892, USA*

Received 9 July 2008; accepted in revised form 5 March 2009; available online 14 March 2009

Abstract

New measurements of Os, He, Sr and Nd isotopes, along with major and trace elements, are presented for basalts from the three volcanic flank zones in Iceland and from Jan Mayen Island. The $^{187}Os/^{188}Os$ ratios in lavas with <30 ppt Os ($n = 4$) are elevated compared to ratios in coexisting olivine and appear to be contaminated at a shallow level. The $^{187}Os/^{188}Os$ ratios in the remaining lavas with >30 ppt Os ($n = 17$) range between 0.12117 and 0.13324. These values are surprisingly low for oceanic island basalts and include some samples that are less than putative present-day primitive upper mantle (PUM with $^{187}Os/^{188}Os$ of 0.1296). These low $^{187}Os/^{188}Os$ preclude significant shallow-level contamination from oceanic crust. The $^{187}Os/^{188}Os$ ratios for Jan Mayen lavas are less than PUM, severely limiting the presence of any continental crust in their mantle source. A positive correlation between $^{143}Nd/^{144}Nd$ and $^{187}Os/^{188}Os$ ratios in Iceland and Jan Mayen lavas likely reflects the presence in their source of ancient subcontinental lithosphere that has undergone incompatible trace element enrichment that did not affect the Re–Os system. In addition, the Jan Mayen lava isotopic signature cannot be explained solely by the presence of subcontinental lithospheric mantle, and the influence of another geochemical component, such as a mantle plume appears required. Combined $^{87}Sr/^{86}Sr$, $^{143}Nd/^{144}Nd$, $^{3}He/^{4}He$ and $^{187}Os/^{188}Os$ data indicate a genetic relationship between Jan Mayen Island and the Iceland mantle plume. Material from the Iceland mantle plume likely migrates at depth until it reaches the tensional setting of the Jan Mayen Fracture Zone, where it undergoes low-degree partial melting. At a first-order, isotopic co-variations can be interpreted as broadly binary mixing curves between two primary end-members. One end-member, characterized in particular by its unradiogenic $^{187}Os/^{188}Os$ and $^{143}Nd/^{144}Nd$, low $^{3}He/^{4}He$ and high $^{87}Sr/^{86}Sr$, is represented by subcontinental lithospheric mantle stranded and disseminated in the upper mantle during the opening of the Atlantic Ocean. The second end-member corresponds to a hybrid mixture between the depleted-MORB mantle and the enriched Iceland mantle plume, itself resulting from mixing between recycled oceanic crust and depleted lower mantle. This hybrid accounts for the high $^{3}He/^{4}He$ (~28 Ra), high $^{143}Nd/^{144}Nd$ (~0.5132), high $^{187}Os/^{188}Os$ (~0.14) and low $^{87}Sr/^{86}Sr$ (~0.7026) composition observed in Iceland. Two different models may account for these observed mixing relationships between the end-members. In this first model, the Iceland mantle entrains pristine depleted material when rising in the upper

* Corresponding author.
E-mail address: vinciane.debaille@ulb.ac.be (V. Debaille).

0016-7037/$ - see front matter
doi:10.1016/j.gca.2009.03.002

mantle and allows refractory sub-lithospheric fragments to melt because of excess heat derived from the deep plume material. A second model that may better account for the Pb isotopic variations observed, uses the same components but where the depleted-MORB mantle is already polluted by subcontinental lithospheric mantle material before mixing with the Iceland mantle plume. Both cases likely occur. Though only three principal components are required to explain the isotopic variations of the Iceland–Jan Mayen system, the different possible mixing relationships may be accounted for by potentially a greater number of end-members.

1. INTRODUCTION

Located on the Mid-Atlantic Ridge, Iceland is generally accepted as the expression of the interaction between a long-lived mantle plume and the Mid-Atlantic Ridge (MAR). Seismic investigations of the Iceland plume stem have been equivocal. For example, Foulger et al. (2001) and Montelli et al. (2004) have indicated that the plume is confined to the upper mantle, while other studies (Helmberger et al., 1998; Bijwaard and Spakman, 1999; Shen et al., 2002; Li et al., 2003; Zhao, 2004; Montelli et al., 2006) found evidence that the plume may originate in the lower mantle, possibly at the core-mantle boundary. However, some authors (e.g., Foulger et al., 2005) still dispute the existence of a mantle plume beneath Iceland. Material from the Iceland plume is clearly dispersed in the shallow upper mantle, as shown by the incompatible trace element (ITE) enriched signature of Atlantic mid-ocean ridge basalts (MORB) progressively decreasing away from Iceland along the MAR (e.g., Schilling, 1973). The geochemical signatures of Icelandic lavas are complex and involve several isotopic end-members. There is a clear ITE-enriched end-member related to the presence of enriched material from the plume. One or more depleted end-members also exist. Some studies have argued for the presence of a depleted end-member that is intrinsic to the upwelling plume, and thus distinct from that within the convecting upper mantle source for Atlantic MORB (e.g., Hémond et al., 1993; Hards et al., 1995; Fitton et al., 1997; Chauvel and Hémond, 2000; Skovgaard et al., 2001; Breddam, 2002; Fitton et al., 2003; Thirlwall et al., 2004; Kokfelt et al., 2006). In contrast, others have argued that the ITE-depleted end-member is indistinguishable from the depleted-MORB mantle (DMM) (Mertz et al., 1991; Haase et al., 1996; Hanan and Schilling, 1997; Hanan et al., 2000; Stracke et al., 2003; Blichert-Toft et al., 2005). Several authors have proposed that the heterogeneity of the Iceland mantle plume can be related to the recycling of the whole section of an oceanic lithosphere, upper altered basaltic crust on one hand, and lower gabbroic oceanic crust plus suboceanic lithosphere on the other hand (Chauvel and Hémond, 2000; Skovgaard et al., 2001; Kokfelt et al., 2006).

Jan Mayen Island (Fig. 1), representing the northern and most elevated part of the Jan Mayen Ridge, is even more enigmatic. The N–S-trending continental fragment of the Jan Mayen Ridge rifted off the Greenland continental shelf following a ridge jump from the extinct Aegir Ridge to the incipient Kolbeinsey Ridge about 30 million years (Ma) ago (Mosar et al., 2002; Breivik et al., 2006). Jan Mayen Island is located in a tensional tectonic setting directly south of the Western Jan Mayen fracture zone (WJMFZ) near the southern termination of the Mohns Ridge (Fig. 1). Some authors (e.g., Haase et al., 1996) have suggested that Jan Mayen volcanism may result from the coincidence of a continental fragment presenting distinct melting characteristics from the surrounding mantle, with the fracture zone and the nearby spreading axis. The continental material would have been left over from the opening of the Atlantic Ocean and dispersed within the upper mantle. However, ITE concentrations of Jan Mayen lavas are not compatible with a depleted-MORB mantle polluted by fragments of continental crust, even though such material in theory could be present owing to the proximal location of the Baltic continental shelf (Trønnes et al., 1999). The $^{176}Hf/^{177}Hf$ compositions of Jan Mayen lavas are also consistent with insignificant contamination by old continental crust (Blichert-Toft et al., 2005).

On the other hand, an isotopic gradient from Jan Mayen along the Kolbeinsey and Mohns Ridges (Schilling et al., 1999), could be ascribed to plume–ridge interaction around Jan Mayen Island, reflecting not only influence of a plume under Jan Mayen, but also its radial dispersion and mixing with the surrounding depleted upper mantle. The "high $^{3}He/^{4}He$" with values of up to 37 Ra (where Ra is the $^{3}He/^{4}He$ of sample normalized to $^{3}He/^{4}He$ atmospheric value of 1.39×10^{-6}) in Iceland lavas, forms a distinct regional zone relative to a "low $^{3}He/^{4}He$" zone in lavas from the Jan Mayen area. These distinct zones imply a weaker or possibly, non-existent, plume system under Jan Mayen that could be independent from the Iceland mantle plume (Schilling et al., 1999). The low $^{3}He/^{4}He$ signal around Jan Mayen Island reflects radiogenic He (6.8–8.1 Ra (Schilling et al., 1999)), suggesting that the enriched source in the sub-North Atlantic may be derived from degassed, possibly recycled material. Low $^{3}He/^{4}He$ (1.5–6 Ra) is also present in the Iceland Northern rift zone (Macpherson et al., 2005) primarily related to degassing, leading to low He concentration and greater sensitivity to contamination by low $^{3}He/^{4}He$ material. Alternatively, the enriched signature of the Jan Mayen and southern Mohns Ridge lavas could reflect the presence of enriched and fertile material emplaced in the northeast Atlantic upper mantle by the ancestral Iceland plume at around 60 Ma (Trønnes et al., 1999).

Icelandic tholeiitic basalts and picrites from the active rift zones reflect a high partial melting degree owing to juxtaposition of the Iceland mantle plume and the Mid-Atlantic Ridge. The Icelandic flank zone volcanism is characterized by mildly alkaline and transitional tholeiitic compositions, that contrast with the predominantly tholeiitic rift zone volcanism (e.g., Sæmundsson, 1979). The

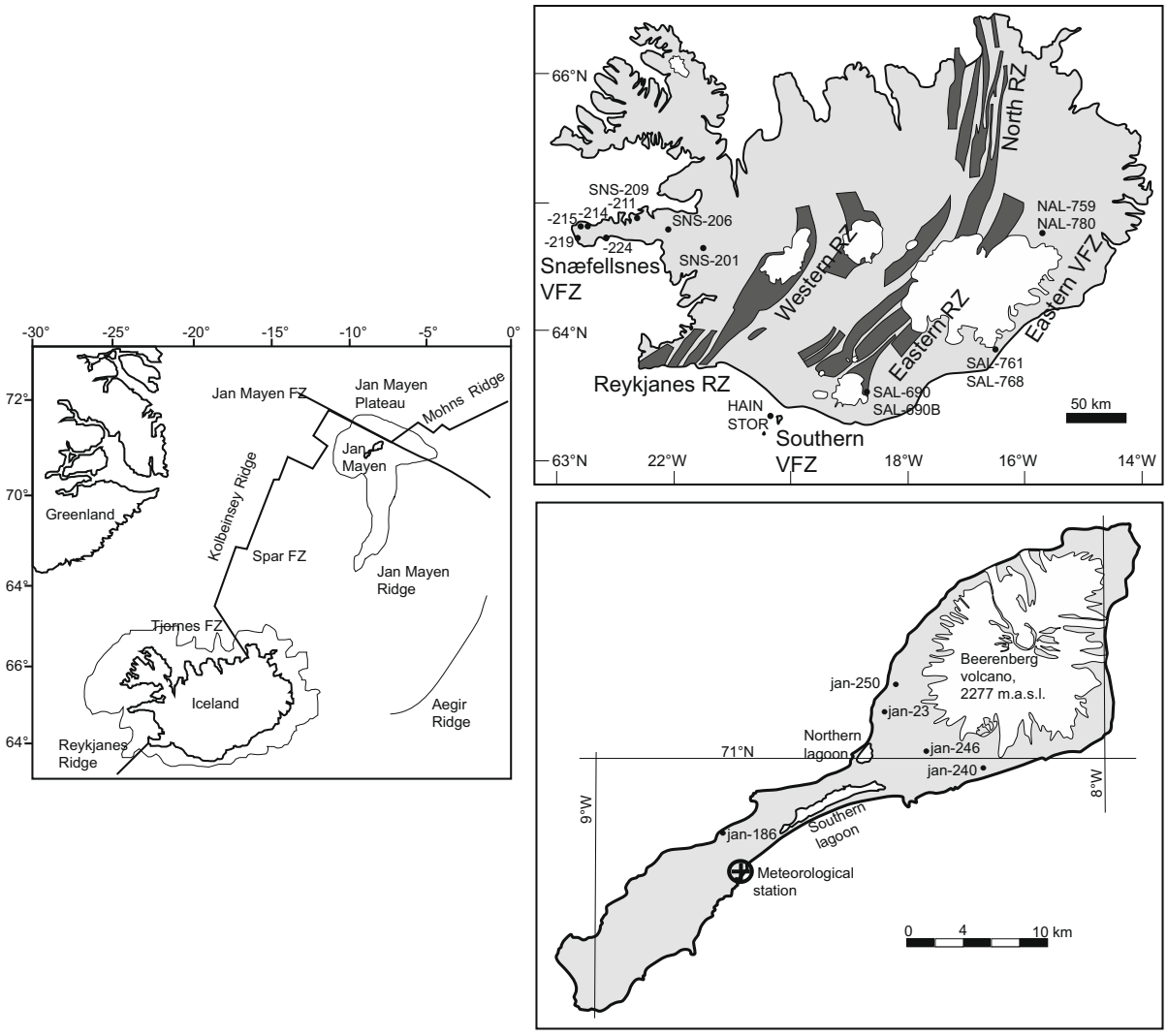

Fig. 1. Map of study area with sample locations indicated by their names, RF for rift zone, VFZ for volcanic flank zone.

eruption of mildly alkaline basaltic lavas is confined to these peripheral flank zone vents on Iceland. Three non-rifting volcanic flank zones (VFZ) have been delineated: the Snaefellsnes Peninsula (SNVFZ) in western Iceland, the Southern Flank Zone (SVFZ) at the tip of the Eastern Rift Zone, and the Eastern Flank Zone (EVFZ) (Fig. 1).

Compared to rift-zone tholeiites, the flank zone basalts are generally enriched in incompatible elements (Nb/Zr > 0.1) and have more radiogenic $^{87}Sr/^{86}Sr$ and $^{206,207,208}Pb/^{204}Pb$ isotopic compositions (e.g., Hémond et al., 1993; Fitton et al., 1997; Chauvel and Hémond, 2000; Stracke et al., 2003; Thirlwall et al., 2004; Kokfelt et al., 2006). In addition, many of the flank zone lavas in Iceland (like the alkaline rocks of Jan Mayen) have MORB-like (~8 Ra) or lower $^{3}He/^{4}He$-ratios (Kurz et al., 1982; Poreda et al., 1986; Sigmarsson et al., 1992). These geographically related heterogeneities could result from different degrees of partial melting related to different crustal thickness (Elliott et al., 1991; Hards et al., 1995; Stracke et al., 1998). The inferred low to moderate degree of partial melting of the mantle under the EVFZ is consistent with the observed crustal thickness of about 30–35 km away from the axial rift zone (Menke et al., 1996; Staples et al., 1997). Alternatively, these trends could also reflect the sampling of a compositionally-zoned Iceland mantle plume (e.g., Fitton et al., 1997; Kempton et al., 2000; Blichert-Toft et al., 2005).

Finally, an EM-1-like signature (Zindler and Hart, 1986), where EM refers to enriched mantle, the number 1 to the origin of enrichment, has been recognized in lavas from Iceland in ^{206}Pb–^{207}Pb–^{208}Pb data (Hanan and Schilling, 1986, 1997; Hanan et al., 2000; Stracke et al., 2003; Blichert-Toft et al., 2005). These authors proposed that this EM-1-like signature is probably related to the presence of subcontinental lithosphere delaminated by convection in the upper mantle during the opening of North Atlantic. Schilling et al. (1999) also suggested that the lack of coherence between the $^{87}Sr/^{86}Sr$, $^{143}Nd/^{144}Nd$, $^{206}Pb/^{204}Pb$, $^{207}Pb/^{204}Pb$ and $^{208}Pb/^{204}Pb$ compositions along the Knipovich Ridge, on the North of Mohns Ridge (Fig. 1) may result from delaminated subcontinental lithosphere randomly dispersed in the underlying mantle and possibly

related to the proximity of Svalbard Archipelago and its deep continental root (Jordan, 1988). This hypothesis is also consistent with the $^{87}Sr/^{86}Sr$, $^{143}Nd/^{144}Nd$, $^{206}Pb/^{204}Pb$, $^{207}Pb/^{204}Pb$ and $^{208}Pb/^{204}Pb$ signature of the Gakkel Ridge (Goldstein et al., 2008).

To further assess possible compositional heterogeneities present in the Iceland mantle plume and to re-assess the origin of Jan Mayen Island within the context outlined above, $^{187}Os/^{188}Os$ ratios of volcanic flank zone lavas from Iceland and Jan Mayen were obtained in this study. In contrast to lithophile isotopic systems such as ^{87}Rb–^{87}Sr, ^{147}Sm–^{143}Nd, $^{235,238}U$–^{232}Th–$^{206,207,208}Pb$ and ^{176}Lu–^{176}Hf, where parent *and* daughter elements display incompatible behavior during partial melting of mantle peridotite and fractionation of basaltic magma, Re and Os display different behaviors during magmatic processes. Rhenium is moderately incompatible while osmium is compatible during partial melting of peridotite, resulting in very high Re/Os in both continental and oceanic crust. Consequently, crustal sources are extremely poor in Os and evolve rapidly to high $^{187}Os/^{188}Os$ relative to sources with no melt enrichment (e.g., Morgan, 1986). Despite the high Re/Os ratios of oceanic crust, because of the contrast in Os concentration between the mantle and the oceanic crust (~3 ppb and ~0.01 ppb, respectively) (Shirey and Walker, 1998), $^{187}Os/^{188}Os$ ratios in the mantle are only sensitive to large percentages of oceanic crust recycling during source mixing (Widom et al., 1999), though this percentage is reduced as the age of recycled oceanic crust increases. Because the compatible behavior of Os during fractional crystallization typically results in evolved basaltic melts with Os concentrations of <0.05 ppb, these melts are sensitive to contamination by surrounding material during their ascent. Continental crust is relatively depleted in Os (~0.05 ppb), but is characterized by large $^{187}Os/^{188}Os$ (typically $\gg 1$), and thus can easily shift the $^{187}Os/^{188}Os$ of evolved basalt melts towards radiogenic values during shallow level contamination processes. On the other hand, subcontinental domains, typically composed of depleted harzburgitic residue, have 10–100 times the Os contents of basalt melts (Widom and Shirey, 1996; Shirey and Walker, 1998) and they can very easily imprint their distinct unradiogenic, and clearly subchondritic $^{187}Os/^{188}Os$ during source mixing. Recently, it has been proposed that the suboceanic lithospheric mantle, i.e., the lowest portion of oceanic lithosphere may also have developed very unradiogenic Os isotope ratios (Bizimis et al., 2007). Because of its unique behavior compared to lithophile element isotopic systems, Os offers new insights to the origin of geochemical variations beneath Iceland and Jan Mayen.

2. SAMPLES

The samples for this study come from the three active volcanic flank zones (VFZ; i.e. non-rifting zones) in Iceland (Southern VFZ, Eastern VZF and Snæfellness VFZ) and from Jan Mayen Island (Fig. 1). The lavas sampled are the most primitive (and olivine-phyric) alkaline to transitional tholeiitic basalts present in their suites (i.e. between 5.2 and 12.4 wt.% MgO).

None of the investigated samples are older than the current Brunhes magnetic epoch (700–800 kilo years (ka)). The samples from Snæfellness VFZ are Holocene, and erupted between 5 and 9 ka, except for SNS214, that erupted during Eem (110–113 ka). Samples SAL690 and SAL690B (700–110 ka) are from the basement of the Katla volcano in the Southern VFZ. The samples from Heimaey Island (HAIN and STOR) erupted at about 10 and 6 ka, respectively (Sigmarsson, 1996; Mattson and Höskuldsson, 2003). Two different units were sampled in the Eastern VFZ. First, the Snæfell volcanic edifice (NAL-759 and -780) which is currently inactive, has normal remnant magnetization (Kristjansson et al., 1988). Second, the Öræfajökull volcanic edifice which is presently active, is represented by SAL761 from the early Holocene (post-glacial, <10 ka), and SAL768 from the Late Pleistocene (100–10 ka, probably less than 50 ka). The samples from Jan Mayen Island are relatively young. JAN-186 and JAN-240 are from the Holocene Inndal formation (<10 ka), and the rest are from the latest Pleistocene Nordvestkapp formation (around 10 ka) (Dallmann et al., 2002).

3. ANALYTICAL TECHNIQUES

The 21 basalts from the Icelandic volcanic flank zones and Jan Mayen Island, as well as 9 olivine and 2 clinopyroxene fractions from selected samples have been analyzed for $^{187}Os/^{188}Os$, and Re and Os concentrations by spiking the samples with a mixed spike enriched in ^{99}Ru–^{105}Pd–^{185}Re–^{190}Os–^{191}Ir–^{198}Pt. The chemical procedures were performed in a clean lab at the Johnson Space Center (JSC). Major and trace elements concentrations and $^{87}Sr/^{86}Sr$ and $^{143}Nd/^{144}Nd$ compositions were measured on separate aliquots.

For platinum group elements (PGE), consisting of Os, Ir, Ru, Rh, Pt and Pd, a procedure was implemented to avoid contamination from metallic pieces. Before manual grinding in agate mortar, lightly crushed samples were sieved in order to extract the 200–500 μm fraction. This is because the fraction under 200 μm was considered as the most prone to have been contaminated, and the fraction over 500 μm would have required additional crushing step, possibly contaminating the samples. This selection resulted in unexpected minor enrichment of olivine and lead to two distinct rock powders, one "normal WR powder" (for major and trace element concentrations, and $^{87}Sr/^{86}Sr$ and $^{143}Nd/^{144}Nd$ measurements), and one olivine-enriched powder (for $^{187}Os/^{188}Os$ and PGE concentrations measurements). Incompatible trace element concentrations have been obtained on both powders, and on purified olivine powder, in order to estimate the percentage and possible effects of olivine enrichment. Assuming that the trace element concentration differences between the two powders result solely from olivine enrichment, the concentrations C of the "normal WR powder" can be calculated according to the equation:

$$C_{accumulated\ rock} = X \times C_{olivine} + (1 - X) \times C_{whole\ rock}$$

where X is the percentage of artificial olivine enrichment.

Using the average calculated percentage of olivine enrichment for each sample obtained from the average value of all incompatible trace elements (Table A1 in Appendix) and the Re and Os concentrations from both powders and olivines, the Re and Os concentrations can be corrected for olivine enrichment during processing. Since the olivine powder may not be absolutely pure and may contain groundmass, this percentage is a maximum value of the artificial olivine enrichment. The variations in Re and Os concentrations resulting from olivine enrichment are between 0 and 39% and 0 and 66%, respectively (Table A2 in Appendix) and within the natural variability shown by the samples (see for example duplicates for SNS209 or SNS214 in Table 1). Hence, the measured values for Re, Os and $^{187}Os/^{188}Os$ are used without any corrections resulting from olivine enrichment.

Table 1
MgO, Mg-number (Mg#), $^{87}Sr/^{86}Sr$, $^{143}Nd/^{144}Nd$ and $^{187}Os/^{188}Os$ isotopic compositions and Os and Re concentrations for basalts from Jan Mayen Island and Iceland volcanic flank zones.

	Latitude (°N)	Longitude (°W)	MgO (wt.%)	Mg#	$^{187}Os/^{188}Os$	Os		Re		$^{87}Sr/^{86}Sr$	$^{143}Nd/^{144}Nd$
					2σ	2RSE		2RSE		2σ	2σ
Jan Mayen Island											
JAN23	71.03	8.43	12.45	0.73	0.12431 ± 11	0.118	1.3	0.232	2.3	0.703439 ± 11	0.512898 ± 8
					0.12508 ± 11	0.179	2.0	0.252	1.4		
						0.125	0.3	0.049	1.6		
JAN186	69.95	8.75	10.47	0.67	0.12582 ± 9	0.070	1.3	0.184	3.0	0.703476 ± 17	0.512881 ± 7
					0.12660 ± 12	0.079	0.2	0.226	1.5		
JAN240	71.00	8.30	11.94	0.72	0.12637 ± 7	0.068	1.5	0.401	4.0	0.703412 ± 15	0.512875 ± 8
JAN246	71.00	8.35	11.31	0.70	0.12665 ± 18	0.084	0.1	0.127	1.5	0.703420 ± 11	0.512890 ± 6
					0.12789 ± 8	0.069	3.7	0.126	4.3		
						0.030	0.5	0.136	1.4		
JAN250	71.05	8.42	6.58	0.55	0.12884 ± 9	0.058	0.4	0.659	1.4	0.703444 ± 13	0.512895 ± 5
					0.12913 ± 12	0.068	1.5	0.601	7.1		
Snaefellness Flank Zone											
Ljósufjöll											
SNS201	64.72	21.98	9.36	0.64	0.13304 ± 9	0.190	4.2	0.306	3.1	0.703228 ± 13	0.512963 ± 9
SNS206	64.89	22.34	9.10	0.63	0.12891 ± 9	0.259	0.8	0.258	1.4	0.703328 ± 13	0.512948 ± 9
SNS209	64.96	22.91	12.35	0.71	0.12738 ± 10	0.190	1.0	0.159	1.6	0.703321 ± 14	0.512938 ± 8
					0.12732 ± 8	0.319	0.5	0.160	1.3		
SNS211	64.96	22.92	10.00	0.67	0.12709 ± 9	0.234	1.7	0.411	2.2	0.703329 ± 15	0.512922 ± 6
Snæfellsjökull											
SNS214	64.90	23.74	9.95	0.65	0.12629 ± 8	0.365	5.1	0.222	2.5	0.703402 ± 13	0.512966 ± 8
						0.095	0.3	0.199	1.1		
SNS215	64.87	23.90	9.74	0.64	0.13256 ± 34	0.073	0.2	0.182	1.4	0.703327 ± 14	0.512961 ± 7
					0.13184 ± 11	0.042	0.9	0.165	2.7		
SNS219	64.87	23.88	9.39	0.63	0.12117 ± 33	0.046	1.0	0.193	2.9	0.703331 ± 11	0.512930 ± 7
						0.064	0.2	0.244	1.1		
SNS224	64.83	23.39	9.97	0.63	0.12587 ± 14	0.049	1.1	0.223	3.5	0.703342 ± 14	0.512977 ± 8
South Flank Zone											
Heimaey											
HAIN	63.67	18.83	9.19	0.62	0.13697 ± 26	0.022	2.4	0.066	5.8	0.703059 ± 15	0.513006 ± 7
						0.014	0.1	0.082	1.8		
STOR	63.67	18.83	10.55	0.65	0.15184 ± 9	0.043	1.9	0.155	4.5	0.703125 ± 13	0.513016 ± 9
					0.15344 ± 33	0.032	0.1	0.165	1.1		
Katla											
SAL690	63.40	20.30	7.48	0.61	0.13690 ± 9	0.027	0.2	0.144	2.2	0.703331 ± 17	0.512923 ± 13
					0.13622 ± 21	0.027	1.5	0.312	1.1		
SAL690B	63.45	20.30	8.40	0.61	0.13324 ± 10	0.042	1.0	0.713	4.2	0.703329 ± 17	0.512975 ± 11
Eastern Flank Zone											
Öræfajökull											
SAL761	63.93	16.48	5.24	0.42	0.175813 ± 14	0.007	2.1	0.391	38.3	0.703688 ± 15	0.512962 ± 11
SAL768	63.90	16.60	6.57	0.54	0.13237 ± 13	0.066	2.8	0.235	6.3	0.703698 ± 11	0.512926 ± 11
Snæfell											
NAL759	64.80	15.57	8.09	0.60	0.12824 ± 16	0.063	0.5	0.582	1.3	0.703346 ± 14	0.512993 ± 7
NAL780	64.80	15.57	9.48	0.65	0.13014 ± 8	0.072	1.6	0.222	3.8	0.703346 ± 18	0.512989 ± 8

Error on MgO is 0.6 – 1.4%. Errors on isotopic measurements (2σ) are on the two last digits. Os and Re concentrations are in ppb. 2RSE (%) is two times the relative standard error.

Aliquots of 1.5–2.5 g of sample powders and mixed PGE spike were dissolved in pre-cleaned quartz carius tubes using inverse aqua regia (3:1 HNO_3:HCl) (Shirey and Walker, 1995), at 230 °C for ⩾48 h. Osmium was extracted using carbon tetrachloride (CCl_4) followed by back extraction into HBr (Cohen and Waters, 1996), and subsequently purified by micro-distillation (Birck et al., 1997). The Os cuts were loaded on 99.999% pure Pt filaments, with a solution of 0.1 M NaOH saturated in $Ba(OH)_2$ and were then measured on a Thermofinnigan Triton at Johnson Space Center, as OsO_3^- in negative mode with a secondary electron multiplier.

The raw Os data were oxygen-corrected using the oxygen isotope composition measured for ReO_4^- (Brandon et al., 2006), followed by instrumental mass fractionation corrections using $^{192}Os/^{188}Os = 3.083$. The mean of 8 Johnson Matthey Os standard measurements, made during the course of analyses, is $^{187}Os/^{188}Os = 0.11377 \pm 29$ (2σ) and within the values previously reported (Brandon et al., 1999, 2000, 2006). Procedural blanks for Os were 1.8 ± 1.5 pg (2σ; $n = 5$) (0.5 pg for minerals). Blank corrections applied to Os concentrations were 0.2–3%, and to $^{187}Os/^{188}Os$ were 0.1–0.8%.

After extraction of Os from the aqua regia, these PGE-bearing solutions were dried down, then re-dissolved twice in 6 N HCl. To purify for PGE, the residues were taken up in 0.15 N HCl and passed three times through a cation column (Neal, 2001). Isotope dilution measurements were performed on a magnetic sector, single-collector ICP-MS (Thermofinnigan Element 2) at Rice University. Samples were introduced into the ICP-MS torch via a microconcentric nebulizer (Cetac MCN-100) (Lee, 2002) in 0.1 N HCl. Mass fractionation was monitored by running a mixed PGE standard at the beginning and the end of each run. The blank background has been subtracted from the sample intensities. The relative internal precision on the Re data is typically of 0.3–7.1% (2RSE (relative standard error)), except for one sample, SAL761 (2RSE = 38%). The total procedural blank for Re is 5.8 ± 5 pg ($n = 5$) (1 pg for the minerals). Blank corrections applied to Re concentrations were 0.8–10%. Results of whole rock and mineral analyses are listed in Tables 1 and 2, respectively. Data for other PGE on these samples will be presented elsewhere as they are not relevant to the issues addressed in this current study.

Analytical procedures for helium are presented in Graham et al. (1998). Olivine separates were analyzed for $^3He/^4He$ by in vacuo crushing using approximately 200 high impact strokes. The reported 2σ errors (Table 3) include in-run analytical uncertainties, plus those associated with air standards and blank corrections.

For $^{87}Sr/^{86}Sr$ analyses, samples were leached for 1 h in hot 6 M HCl prior to dissolution. After dissolution, they were processed over conventional cation exchange columns and then further purified using Sr-spec resin. Samples were loaded on Ta filaments with H_3PO_4 and TaF activator. $^{87}Sr/^{86}Sr$ measurements were carried out in dynamic mode on a VG sector 54 TIMS at the Geological Institute, University of Copenhagen. The average value of SRM987 standard obtained over the period of analysis was $^{87}Sr/^{86}Sr = 0.710232 \pm 22$ ($n = 8$). Blanks were less than 300 pg.

The $^{143}Nd/^{144}Nd$ isotopic analyses were carried out on a bulk REE cut collected off conventional cation exchange columns followed by REE purification on HDEHP columns using the same dissolution as used for Sr analyses. Analyses were run on an Axiom MC-ICPMS at the Danish Lithosphere Centre, Copenhagen using methods similar to those described by Luais et al. (1997). Average value of DLC/Ames mixed Sm/Nd Ames standard was $^{143}Nd/^{144}Nd = 0.512132 \pm 11$ ($n = 23$) and average value of La Jolla Nd standard was $^{143}Nd/^{144}Nd = 0.511843 \pm 10$ ($n = 2$). Blanks were less than 50 pg. $^{87}Sr/^{86}Sr$ and $^{143}Nd/^{144}Nd$ results are presented in Table 1.

The major and trace element concentrations were analyzed by XRF and ICP-MS at Activation Laboratories, Ancaster, Ontario, using 3 and 2 blind parallels of the international reference standards BHVO-1 and BCR-1, respec-

Table 2
Isotopic compositions, concentrations and partition coefficients for olivines and clinopyroxenes for basalts from Jan Mayen Island and Iceland volcanic flank zones.

	187Os/188Os 2σ	Os 2RSE	Re 2RSE	$K_{DOs}^{mineral/melt}$	$K_{DRe}^{mineral/melt}$
Ol JAN23	0.12446 ± 26	0.079 ± 1.5	0.012 ± 8.8	0.67	0.05
Ol JAN246	0.12559 ± 45	0.032 ± 1.0	0.034 ± 8.4	0.38	0.27
Ol NAL759	0.12920 ± 19	0.024 ± 0.5	0.038 ± 5.5	0.38	0.07
Ol SAL690	0.13217 ± 32	0.024 ± 0.7	0.114 ± 4.7	0.87	0.79
Ol SAL768	0.13431 ± 91	0.010 ± 0.3	0.097 ± 5.3	0.15	0.41
Ol SNS201	0.13169 ± 8	0.730 ± 18.6	0.082 ± 4.0	3.84	0.27
Ol SNS209	0.12743 ± 11	0.102 ± 3.1	0.079 ± 4.4	0.54	0.50
Ol SNS214	0.12751 ± 9	0.094 ± 2.6	0.038 ± 5.7	0.26	0.17
Ol HAIN	0.13147 ± 19	0.015 ± 0.4	0.007 ± 10.7	0.65	0.11
			Average K_D in olivine	<u>0.86</u>	<u>0.29</u>
Au JAN23	0.12509 ± 111	0.012 ± 0.4	0.069 ± 4.2	0.10	0.30
Di JAN23	0.12645 ± 15	0.020 ± 0.6	0.025 ± 5.0	0.17	0.11
			Average K_D in pyroxene	<u>0.13</u>	<u>0.20</u>

Os and Re concentrations are in ppb. Average values for Os and Re partition coefficients (K_D) in olivine and pyroxene (Au: augite and Di: diopside), respectively, are underlined. 2RSE (%) is two times the relative standard error.

Table 3
$^{3}He/^{4}He$ (R/Ra) and He concentrations in olivines for basalts from Jan Mayen Island and Iceland volcanic flank zones.

Sample	Weight (g)	Phase	$^{3}He/^{4}He$ (R/Ra)	2σ	[He] (ccSTP/g)
JAN23	431.8	Olivine	6.15	±0.22	4.10E−09
JAN240	480.5	Lt olivine	6.60	±0.15	8.80E−09
JAN240	326.4	Dk olivine	6.02	±0.14	1.86E−08
JAN246	603.6	Lt olivine	6.61	±0.13	1.48E−08
JAN-250	400.2	Lt olivine	6.36	±0.25	5.59E−09
HAIN	469.1	Olivine	11.05	±0.37	2.95E−09
SAL690	460.8	Olivine	16.78	±0.24	1.07E−08
SAL690B	661.6	Olivine	18.06	±0.32	4.75E−09
SAL768	516.8	Olivine	7.69	±0.12	1.36E−08
NAL759	441.6	Olivine	7.06	±0.17	8.58E−09

All helium analyses by in vacuo crushing using ~200 high impact strokes. 2σ errors include in-run analytical uncertainties, plus those associated with air standards and blank corrections. Dk and lt for dark and light olivine, respectively.

tively, for monitoring the analytical precision and accuracy. The parallel and standard samples were randomly located in the sequentially numbered series of sample powders. The precision and accuracy are roughly similar and estimated to 0.6–1.4% for the major element oxides, except Na_2O, K_2O, P_2O_5 (1.8, 7.7 and 5.6%, respectively). The corresponding uncertainties are less than 3% for Sr, Ba, REE, Hf and U and less than 9% for the rest of the elements. Results are presented in Table 4 for trace element concentrations and Tables 1 and A3 for major element contents.

4. RESULTS

The samples from Iceland volcanic flank zones and Jan Mayen Island analyzed in this study are alkaline to transitional tholeiitic basalts with MgO ranging from 5.2 to 12.4 wt.%. The Os and Re concentrations vary from 7 to 365 ppt and from 55 to 715 ppt, respectively. The Iceland VFZ samples range in $^{187}Os/^{188}Os$ from 0.12117 to 0.17581 ($\gamma_{Os} = -4.6$ to 38). Jan Mayen samples have a more restricted range from 0.12431 to 0.12913 ($\gamma_{Os} = -2.1$ to 1.7). Because of the young but imprecise ages of the samples from both islands that are between 700 ka and present, the $^{187}Os/^{188}Os$ ratios are not corrected for ^{187}Os in-growth. This may result in overestimating the $^{187}Os/^{188}Os$ by 0.5% in the worst case (sample SAL690B, assuming a maximum age of 700,000 years). The Jan Mayen lavas and 6 VFZ lavas from Iceland have $^{187}Os/^{188}Os$ lower than the putative present-day primitive upper mantle (PUM) at 0.1296 ± 0.008 (Meisel et al., 2001). This is generally not observed in the global database of ocean-island basalts. In particular, samples with subchondritic $^{187}Os/^{188}Os$ (<0.127) are virtually absent (see for example the OIB compilation in Shirey and Walker (1998)). Only 13 basalts from the Pico, Faial and Terceira Islands (Azores Islands) have $^{187}Os/^{188}Os$ from 0.11019 to 0.127 (Widom and Shirey, 1996; Schaefer et al., 2002), and also some mantle xenoliths from Kerguelen (Hassler and Shimizu, 1998) and Hawaii (Bizimis et al., 2007).

The Os concentrations have a broadly negative correlation with $^{187}Os/^{188}Os$ (Fig. 2). The range in $^{187}Os/^{188}Os$ of 0.12117–0.17581 is present at concentrations of 0.007–0.365 ppb, where the sample with the highest $^{187}Os/^{188}Os$ of 0.17581 (SAL761), has the lowest MgO and Os concentrations of 5.24% and 0.007 ppb, respectively. The Snæfellness VFZ and Jan Mayen samples have an $^{187}Os/^{188}Os$ range of 0.12117–0.13304 throughout almost their full Os concentration range of 0.030–0.365 ppb (Table 1 and Fig. 2). Discrepancy between $^{187}Os/^{188}Os$ of the olivines and their corresponding whole-rocks is lower than 1.5%, except for two samples, HAIN and SAL690 (4 and 3.5%, respectively), which also have low Os concentrations (<40 ppt). Large variations in Os and Re contents between duplicates can be observed for some samples. This is typical of elements strongly influenced by a nugget effect, i.e., the presence of very small sulphide grains in variable quantity that are extremely rich in PGE.

There is no clear correlation between the Re/Os values and MgO wt.% (Fig. 3a), indicating that the behavior of these elements is governed not only by variable fractional crystallization and accumulation of mainly olivine, but also by possible loss of Re due to its volatile behavior (Bennett et al., 2000; Lassiter, 2003). The $^{187}Os/^{188}Os$ values are almost constant for a large variation range of MgO from 5.2 to 12.4 wt.% (Fig. 3b), and for other differentiation indices (not shown), precluding assimilation of radiogenic $^{187}Os/^{188}Os$ material during crystallization, except for the sample SAL761, which has the highest $^{187}Os/^{188}Os$ (0.17581) and the lowest MgO wt.% (5.24%). The high Re/Os of this sample (54.4) is consistent with the near-compatible behavior of Os (average K_D of 0.86, Table 2) and incompatible behavior of Re (average K_D of 0.29, Table 2) in olivine during magmatic processes. Both Os and Re are incompatible in clinopyroxene (average K_D of 0.13 and 0.2, respectively, Table 2). Finally, there is no correlation between Re/Os and $^{187}Os/^{188}Os$ (Fig. 3c), also indicating that $^{187}Os/^{188}Os$ ratios are not influenced to a first-order by assimilation of crustal material during fractional crystallization processes.

The Jan Mayen and VFZ Iceland lavas have $^{87}Sr/^{86}Sr$ and $^{143}Nd/^{144}Nd$ from 0.703059 to 0.703698 and from 0.513016 to 0.512875, respectively (Fig. 4b). These $^{87}Sr/^{86}Sr$ and $^{143}Nd/^{144}Nd$ compositions are generally higher and lower (with some overlap), respectively, than those from Iceland rift zones (e.g., Hémond et al., 1993; Thirlwall et al., 2004), but lie within the well-known trend displayed

Table 4
Trace element concentrations for basalts from Jan Mayen Island and Iceland volcanic flank zones.

	Rb	Ba	Th	U	Nb	Ta	La	Ce	Pr	Sr	Nd	Sm	Zr	Hf	Eu	Gd	Tb	Dy	Ho	Er	Tm	Yb	Lu
Jan Mayen Island																							
JAN23	32.3	537	2.87	0.79	33.6	2.70	27.8	56.7	6.41	457	25.3	4.53	135	3.18	1.49	3.88	0.56	3.10	0.56	1.48	0.21	1.26	0.19
JAN186	31.5	574	3.15	0.81	36.6	2.75	32.0	64.3	7.31	644	29.6	5.80	157	3.65	1.91	5.03	0.74	4.03	0.73	1.96	0.28	1.62	0.23
JAN240	31.3	521	3.25	0.86	37.4	2.93	32.9	65.1	7.33	458	28.4	5.09	142	3.44	1.56	4.29	0.64	3.38	0.63	1.67	0.24	1.38	0.21
JAN246	31.8	542	3.36	0.87	40.9	2.98	32.8	65.9	7.45	458	29.7	5.37	147	3.59	1.66	4.51	0.65	3.53	0.65	1.72	0.24	1.43	0.21
JAN250	55.6	860	5.11	1.38	61.4	4.71	49.6	97.8	11.0	667	41.8	7.13	219	5.04	2.20	5.91	0.85	4.53	0.82	2.19	0.31	1.86	0.27
Snæfellness Flank Zone																							
SNS201	8.11	110	0.91	0.29	13.8	0.79	11.1	25.6	3.25	243	14.6	3.49	91.0	2.35	1.27	3.72	0.60	3.67	0.76	2.19	0.32	1.88	0.28
SNS206	12.3	199	1.58	0.49	23.5	1.63	21.4	47.8	5.86	353	25.3	5.44	126	2.97	1.84	5.32	0.81	4.59	0.90	2.51	0.36	2.06	0.31
SNS209	15.8	219	1.90	0.57	24.9	1.80	20.8	44.1	5.22	331	21.6	4.42	120	2.90	1.47	4.12	0.62	3.43	0.68	1.90	0.27	1.63	0.24
SNS211	21.0	293	2.45	0.76	31.4	2.24	28.1	60.0	7.14	416	29.6	5.83	160	3.57	2.04	5.24	0.78	4.35	0.81	2.22	0.32	1.91	0.29
SNS214	21.1	346	2.26	0.64	34.7	2.45	28.2	59.3	6.91	487	28.6	5.57	164	3.56	1.96	4.94	0.71	3.93	0.73	2.00	0.29	1.75	0.26
SNS215	13.8	350	1.52	0.46	30.3	2.05	25.5	54.8	6.51	432	27.8	5.51	150	3.18	2.01	5.08	0.75	4.10	0.78	2.11	0.30	1.81	0.27
SNS219	13.0	361	1.56	0.47	31.1	2.14	26.6	57.9	6.98	437	29.1	5.76	152	3.39	2.14	5.27	0.77	4.13	0.80	2.14	0.31	1.82	0.28
SNS224	16.7	314	1.75	0.54	31.5	2.16	25.6	55.3	6.60	427	27.7	5.57	150	3.36	1.94	5.03	0.74	4.13	0.79	2.13	0.31	1.81	0.27
South Flank Zone																							
HAIN	13.7	187	2.04	0.67	23.0	1.56	20.5	46.0	5.68	359	23.7	5.47	201	4.60	1.71	5.51	0.84	4.76	0.89	2.43	0.35	2.13	0.31
STOR	9.79	128	1.38	0.47	19.3	1.28	15.9	37.1	4.65	323	20.6	4.84	152	3.64	1.71	5.07	0.77	4.48	0.86	2.27	0.32	1.88	0.28
SAL690	9.90	119	0.95	0.33	13.9	0.91	11.8	28.0	3.66	304	16.4	4.13	131	3.15	1.47	4.71	0.74	4.48	0.88	2.41	0.35	2.13	0.32
SAL690B	6.48	79.2	0.68	0.24	10.3	0.61	8.43	20.9	2.84	239	13.6	3.65	104	2.55	1.33	4.13	0.67	4.21	0.85	2.33	0.34	2.00	0.31
Eastern Flank Zone																							
SAL761	11.7	159	1.38	0.45	16.2	1.18	15.6	36.7	4.83	294	22.0	5.55	168	4.18	2.01	6.34	1.02	6.12	1.21	3.35	0.48	2.86	0.43
SAL768	8.22	127	0.97	0.31	12.9	0.87	11.3	26.3	3.47	343	15.7	3.89	116	2.80	1.44	4.41	0.69	4.15	0.81	2.20	0.31	1.81	0.26
NAL759	15.1	192	1.62	0.50	18.5	1.30	17.2	37.8	4.63	362	20.4	4.62	141	3.36	1.59	4.80	0.72	4.10	0.79	2.12	0.30	1.76	0.27
NAL780	9.12	143	1.17	0.34	14.7	1.01	13.3	29.8	3.75	347	16.4	3.82	114	2.75	1.39	3.88	0.61	3.41	0.65	1.70	0.24	1.40	0.22

Trace elements concentrations are in ppm. The corresponding uncertainties are less than 3% for Sr, Ba, REE, Hf and U and less than 9% for the rest of the elements.

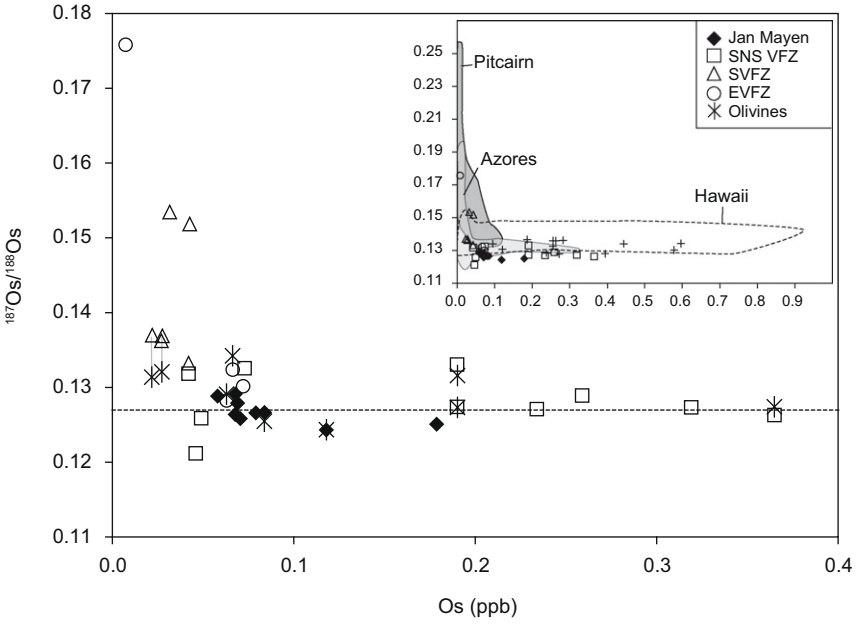

Fig. 2. $^{187}Os/^{188}Os$ vs. Os concentration diagram. Black diamond: Jan Mayen Island; white squares: Snaefellsness VFZ; white triangle: Southern VFZ; white circle: Eastern VFZ. Star: olivines $^{187}Os/^{188}Os$ ratios vs. the Os concentration of the corresponding whole rock. A discrepancy between the $^{187}Os/^{188}Os$ of the whole rocks and the olivines (grey line) is only observed for Os concentrations <30 ppt. Cross: Iceland Os literature data (Brandon et al., 2007). Data for Azores from Widom and Shirey (1996); for Hawaii from Lassiter and Hauri (1998); for Pitcairn from Eisele et al. (2002). Chondritic value of $^{187}Os/^{188}Os$ (Luck and Allègre, 1983; Walker and Morgan, 1989) is represented by dashed line.

by all the Iceland samples and Jan Mayen (Fig. 4b) (e.g., Zindler et al., 1979; Condomines et al., 1983; Elliott et al., 1991; Nicholson et al., 1991; Sigmarsson et al., 1991, 1992; Hémond et al., 1993; Kerr et al., 1995; Kempton et al., 2000; Prestvik et al., 2001; Stracke et al., 2003; Thirlwall et al., 2004; Kokfelt et al., 2006). The new samples from this study confirm that the Jan Mayen and Iceland systems are intrinsically heterogeneous, broadly defining at least two or more chemical components in their mantle sources; those having enrichment, with relative long-term high Rb/Sr and low Sm/Nd, and those that underwent depletion with relative long-term low Rb/Sr and high Sm/Nd (Kerr, 1995; Thirlwall, 1995; Fitton et al., 1997; Chauvel and Hémond, 2000; Kempton et al., 2000; Kokfelt et al., 2006; Brandon et al., 2007). The Jan Mayen lavas have $^{87}Sr/^{86}Sr$ and $^{143}Nd/^{144}Nd$ that cluster near 0.70344 and 0.51289, respectively, that define an enriched component. The $^{87}Sr/^{86}Sr$ and $^{143}Nd/^{144}Nd$ variation in Iceland is geographically delineated. Lavas from the main rift zones, which are more volcanically active, have more of the depleted and tholeiitic compositional component(s) with low $^{87}Sr/^{86}Sr$ (from ~0.70265 to ~0.70326) and high $^{143}Nd/^{144}Nd$ (from ~0.51296 to ~0.51320) (e.g., Thirlwall et al., 2004) (Fig. 4b). The less volcanically active volcanic flank zones have more of the enriched and alkaline compositional component(s) with high $^{87}Sr/^{86}Sr$ (from ~0.7031 to ~0.7035) and low $^{143}Nd/^{144}Nd$ (from ~0.51288 to ~0.51302) (e.g., Hémond et al., 1993; Hards et al., 2000; Thirlwall et al., 2004; Kokfelt et al., 2006; this study). All the samples are light rare earth element (LREE) enriched with La/Sm ratios normalized to CI (Anders and Grevesse, 1989) between 1.45 and 4.36. The Jan Mayen samples have higher ratios (3.46–4.36) than the Iceland volcanic flank zone samples (1.45–3.17).

Helium isotope ratios in lavas from this study range from 6.02 to 18.06 Ra. Jan Mayen lavas have $^{3}He/^{4}He$ between 6.02 and 6.61 Ra, below typical MORB values of 7–9 Ra (Graham, 2002), in agreement with previous work (Schilling et al., 1999). High $^{3}He/^{4}He$ occurs in the Southern VFZ (16.78 ± 0.24 to 18.06 ± 0.32 Ra). Despite the volcanic flank zones extending to lower $^{3}He/^{4}He$ (<8 Ra) compared to the rift zones (8–21 Ra (Breddam et al., 2000; Macpherson et al., 2005; Brandon et al., 2007), there is a large overlap between the two groups.

The new samples from Jan Mayen and the Iceland volcanic flank zones define a broad negative correlation (hyperbola) between $^{87}Sr/^{86}Sr$ and $^{187}Os/^{188}Os$ (Fig. 4c), and a broad positive correlation between $^{143}Nd/^{144}Nd$ and $^{187}Os/^{188}Os$ (Fig. 4a). Finally, there is a positive correlation between $^{187}Os/^{188}Os$ and $^{3}He/^{4}He$ (Fig. 4d), where the Jan Mayen lavas display the most radiogenic $^{3}He/^{4}He$ of ~6 Ra. The new samples define the lower part of the $^{187}Os/^{188}Os$ vs. $^{3}He/^{4}He$ trend already observed in Iceland rift zone picrites (Brandon et al., 2007). This observation is also in agreement with a study of Jackson et al. (2008), except for 5 points that are out of the trend (Fig. 4d).

5. DISCUSSION

5.1. Shallow-level contamination

In order to identify the origin of mantle source signatures underneath Jan Mayen and Iceland, the question of shallow-level contamination has to be addressed first,

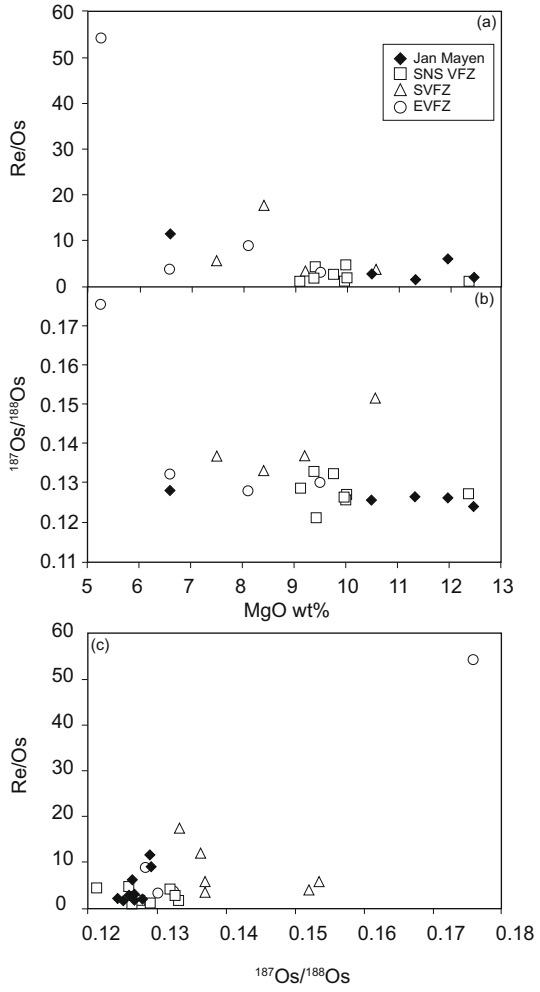

Fig. 3. (a) Re/Os and (b) $^{187}Os/^{188}Os$ vs. MgO content. (c) Re/Os vs. $^{187}Os/^{188}Os$. Same symbols as in Fig. 2. All the samples from the data set are represented.

because of the potential sensitivity of ^{187}Re–^{187}Os systematics to contamination processes. As noted earlier, the new data for lavas from Jan Mayen and the Iceland volcanic flank zones display a negative correlation between $^{187}Os/^{188}Os$ and Os concentration typical for OIB (Fig. 2). The lavas with low Os concentrations (<40 ppt) are generally higher in $^{187}Os/^{188}Os$ than the lavas with Os concentrations >40 ppt, potentially reflecting a susceptibility to minor shallow-level contamination by seawater-derived Os and/or assimilation of small amounts of ocean floor sediments (Reisberg et al., 1993; Martin et al., 1994).

However, olivine crystals are unlikely to have been contaminated by such shallow processes. Comparing the available $^{187}Os/^{188}Os$ between olivine and whole-rocks (Tables 1 and 2 and Fig. 2), a discrepancy is only observed for samples with Os contents <30 ppt (SAL690 and HAIN). In this study, the concentration of 30 ppt is thus taken as a cut-off value for samples that have potentially suffered shallow-level contamination and do not reflect mantle source signatures. Consequently, four samples are eliminated from the data set as potentially modified by shallow level contamination of Os: SAL690, HAIN, SAL761 and STOR. For the last sample, STOR, the low Os concentration of the duplicate (32 ppt) and high $^{187}Os/^{188}Os$ of 0.15184, compared to the average near-chondritic values of the remainder of the data set eliminate this sample. In addition, HAIN and STOR are from Heimaey Island, which is known for its phreatomagmatic eruptions. Hence, sea-water contamination is likely to explain their more radiogenic $^{187}Os/^{188}Os$ than for samples where seawater was not as accessible to the magma conduit systems ($^{187}Os/^{188}Os$ of sea water about 1, (Levasseur et al., 1998)). Sample SAL690B has a low Os content of 42 ppt, with the highest $^{187}Os/^{188}Os$ of the remaining data set (0.13324) but in absence of clear evidence of shallow crustal contamination, has been retained in the discussion of mantle properties.

Because the Re–Os isotopic system is sensitive to crustal contamination particularly for evolved basalt melts with low Os concentrations where very small amounts of assimilation shift the $^{187}Os/^{188}Os$ to more radiogenic values, it thus seems inconsistent to invoke crustal contamination for the samples with subchondritic and slightly superchondritic $^{187}Os/^{188}Os$. Consequently, it is argued that the data presented in this study (excluding the four samples previously described) have escaped significant late-stage contamination and instead reflect mantle source signatures.

With the exception of two samples from Öræfajökull, $^{87}Sr/^{86}Sr$ and $^{143}Nd/^{144}Nd$ data display a negative correlation (Fig. 4b). One Öræfajökull sample, SAL761, was considered above to have been affected by shallow level contamination with respect to $^{187}Os/^{188}Os$, but the second one, SAL768 does not show $^{187}Os/^{188}Os$ evidence for shallow level contamination. Previous studies (Sigmarsson et al., 1992; Prestvik et al., 2001; Kokfelt et al., 2006) have already identified anomalously high Sr isotope ratios ($^{87}Sr/^{86}Sr = \sim 0.7037$) in the Öræfajökull area compared to the rest of Iceland. On the basis of $\delta^{18}O$, Sigmarsson et al. (1992) conclude that contamination by either crust or sea water is unlikely to explain these radiogenic Sr isotope ratios, which may then represent a mantle source signature. More recently, Prestvik et al. (2001) showed that the Pb isotopic composition of the Öræfajökull samples can be explained by a distinct mantle source. Similarly, Kokfelt et al. (2006) proposed that the Öræfajökull source region may contain pelagic sediments recycled with oceanic crust into the mantle source region. Since the relatively high $^{87}Sr/^{86}Sr$ ratio of 0.703698 is thus likely due to source heterogeneity, SAL768 has also been retained in the discussion.

5.2. Relationship between Jan Mayen Island and Iceland

As mentioned earlier, an alternative hypothesis to the presence of a mantle plume beneath Jan Mayen Island (related or not to the Iceland mantle plume) could be melting of ITE-enriched and volatile-rich material resulting from the juxtaposition of a continental fragment consisting of crust and/or subcontinental lithospheric mantle (SCLM), a fracture zone, and the spreading ridge (Haase et al., 1996). Contrasts in Os contents and $^{187}Os/^{188}Os$ ratios between both the continental crust and the SCLM, and the magmas issued from the depleted-MORB mantle

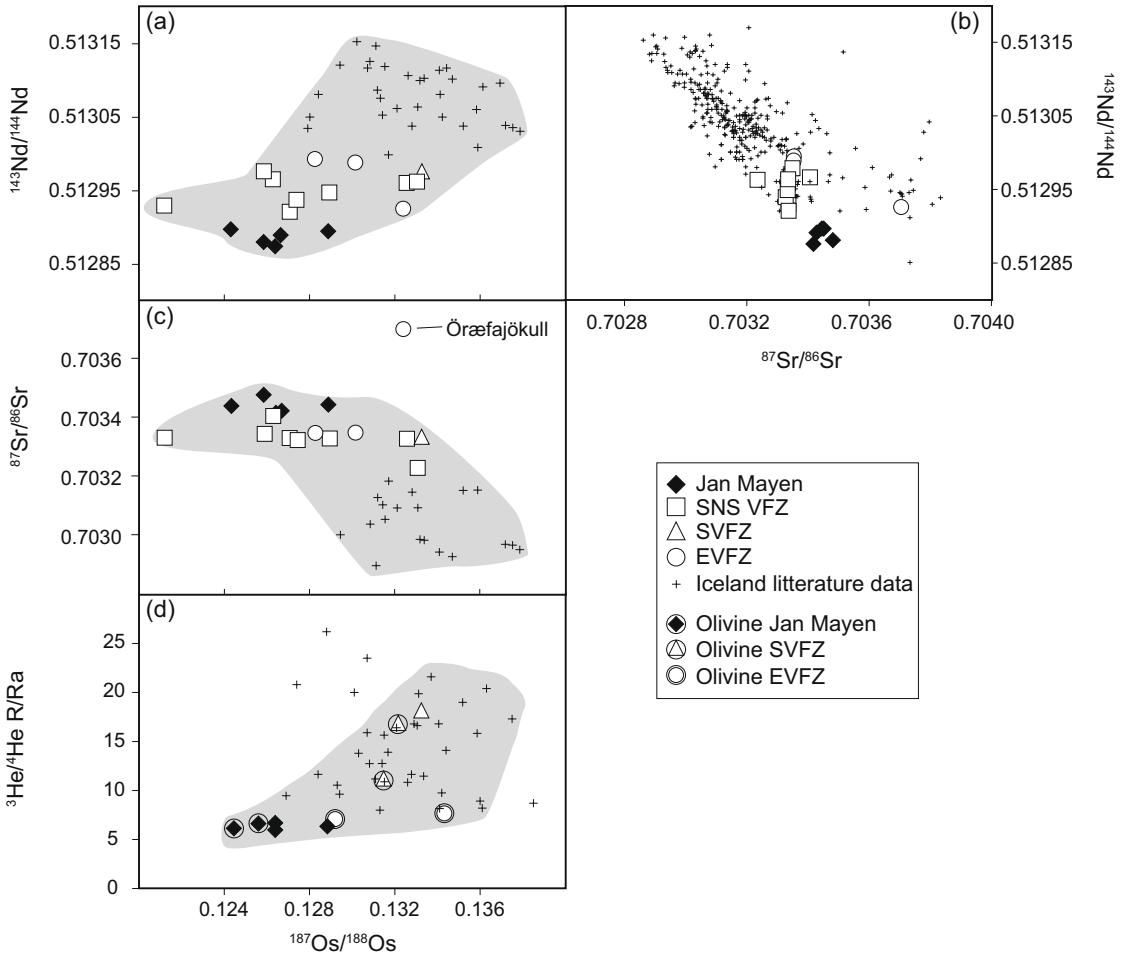

Fig. 4. (a) $^{143}Nd/^{144}Nd$ vs. $^{187}Os/^{188}Os$, (b) $^{143}Nd/^{144}Nd$ vs. $^{87}Sr/^{86}Sr$ and (c) $^{87}Sr/^{86}Sr$ vs. $^{187}Os/^{188}Os$ for whole-rocks samples from this study (except the four samples that have been shown being affected by shallow-level contamination; see text for more details), (d) $^{3}He/^{4}He$ (R/Ra) vs. $^{187}Os/^{188}Os$ where circle superimposition indicates that $^{187}Os/^{188}Os$ has been obtained on olivine separate, instead of whole-rock powder (same symbols as in Fig. 2). The $^{3}He/^{4}He$ data have been measured on olivines. Cross: literature data (Zindler et al., 1979; Condomines et al., 1983; Macdonald et al., 1987; Elliott et al., 1991; Furman et al., 1991; Nicholson et al., 1991; Sigmarsson et al., 1991, 1992, 2000; Hémond et al., 1993; Hards et al., 1995; Fitton et al., 1997; Gee et al., 1998; Chauvel and Hémond, 2000; Hards et al., 2000; Kempton et al., 2000; Steinthorsson et al., 2000; Prestvik et al., 2001; Skovgaard et al., 2001; Breddam, 2002; Stracke et al., 2003; Thirlwall et al., 2004; Kokfelt et al., 2006; Brandon et al., 2007; Jackson et al., 2008); Table A4.

are large. Consequently, a small amount of continental material would significantly shift the $^{187}Os/^{188}Os$ composition of magmas, towards highly radiogenic values if the contaminant is continental crust or towards extremely unradiogenic values in the case of SCLM. The addition of continental crustal material (i.e., $^{187}Os/^{188}Os$ around 1.05 (Peucker-Ehrenbrink and Jahn, 2001)) cannot account for the chondritic to subchondritic $^{187}Os/^{188}Os$ of the Jan Mayen Island samples. In contrast, entrainment of old subcontinental lithospheric mantle in the magma source could potentially result in lower $^{187}Os/^{188}Os$ because SCLM typically has $^{187}Os/^{188}Os$ between 0.102 and 0.116, (e.g., Walker et al., 1989; Shirey and Walker, 1998). However, SCLM with low $^{187}Os/^{188}Os$ (resulting from removal of Re in the distant past) is typically a harzburgitic residue of partial melting. Such refractory peridotite is unlikely to further melt through adiabatic decompression under normal conditions (Arndt and Christensen, 1992). Jan Mayen Island is located at the northernmost end of the Jan Mayen Ridge and JM Platform, with basalts formed by low-degree partial melting (between 8 and 14% on the Mohns Ridge and Jan Mayen Platform, compared to 11–24% on the Kolbeinsey Ridge (Schilling et al., 1999). This makes the presence of a thermal anomaly or volatile enrichment unlikely beneath Jan Mayen, and hence the melting of harzburgitic lithosphere petrologically difficult.

However, the presence of a nearby hotspot could potentially explain the isotopic signature observed at Jan Mayen, by providing the heat required to melt harzburgitic SCLM. While seismic, tectonic, petrological and geochemical evidence (Havskov and Atakan, 1991; Haase et al., 1996; Mertz et al., 2004) seem to argue against the presence of a hotspot underneath Jan Mayen, and there is no systematic age progression of volcanism leading away from the island (Mertz et al., 2004), the values for $^{87}Sr/^{86}Sr$ and $^{143}Nd/^{144}Nd$ of the Jan Mayen samples lie at one extremity

of the Iceland trend (Fig. 4b). This is consistent with a physical/geochemical relationship between the Icelandic plume and Jan Mayen. It would be fortuitous (though not impossible) that a separate but geographically close Jan Mayen component would lie exactly at one extremity of the trend for Iceland in $^{87}Sr/^{86}Sr$–$^{143}Nd/^{144}Nd$–$^{187}Os/^{188}Os$–$^{3}He/^{4}He$ space without sharing a compositional end-member. Although Jan Mayen lavas do not represent an end-member of the Iceland field in the $^{206,207,208}Pb/^{204}Pb$ space, they do show very similar values compared to the volcanic flank zone lavas (Trønnes et al., 1999). In addition, Mertz et al. (2004) have found that the trace element concentrations of off-axis Eggvin Bank (on the West of Jan Mayen Island), as well as the Jan Mayen platform and Jan Mayen Island display a similarity to HIMU (high μ ($=^{238}U/^{204}Pb$)) lavas, while a HIMU geochemical signature has been identified in Iceland (Thirlwall, 1995, 1997; Kokfelt et al., 2006). The very similar normalized incompatible trace element patterns (Fig. 5) of both Jan Mayen samples and Iceland volcanic flank zones indicate a comparable mineralogical and geochemical constitution for their mantle source. The higher concentration of incompatible trace elements in Jan Mayen lavas can easily be explained by lower partial melting degree beneath the island, as previously proposed by Trønnes et al. (1999). If a physical/geochemical relationship exists between the sources of magmas from both islands, Jan Mayen represents the enriched (high $^{87}Sr/^{86}Sr$, low $^{143}Nd/^{144}Nd$) extremity similarly to the volcanic flank zones.

To reconcile the presence of a mantle plume geochemical signature (long-term enrichment in incompatible trace elements) without the physical expression of hotspot volcanism, it has been proposed that the upper mantle beneath Jan Mayen and the NE Atlantic was emplaced by the Iceland plume head during the early Tertiary (Trønnes et al., 1999; Mertz et al., 2004). As argued below, the current lateral flow of Iceland plume material may also provide considerable dispersal of this geochemical signature.

The Mid-Atlantic Ridge between Iceland and Jan Mayen is a complex system, in which fracture zones seem to delineate distinct geochemical domains. Furthermore, there appears to be asymmetric dispersion of both enriched and depleted signatures of the Iceland plume, revealing a heterogeneous structure (zoning) within the Iceland plume (Blichert-Toft et al., 2005). It was initially proposed that the Tjörnes FZ (see Fig. 1) acts as a dam, preventing the northward dispersion of the plume (Schilling et al., 1983; Mertz et al., 1991). More recently, an extensive $^{87}Sr/^{86}Sr$–$^{143}Nd/^{144}Nd$–$^{206,207,208}Pb/^{204}Pb$–$^{3}He/^{4}He$ isotope study by Schilling et al. (1999) has revealed a steep $^{206,207,208}Pb/^{204}Pb$ gradient decreasing from Iceland across the Tjörnes Transform Zone and reflecting a northward dispersion of mantle plume material from Iceland. Blichert-Toft et al. (2005) observed the same geochemical gradient when using principal component analysis, but only for the enriched signature of the Iceland plume. It thus does not seem that Tjörnes or Spar FZ act as barrier for the mantle plume flow dispersed along the Kolbeinsey ridge. The Jan Mayen Fracture Zone, however, represents a major geochemical boundary between the Kolbeinsey Ridge and the southern part of the Mohns Ridge in terms of $^{206,207,208}Pb/^{204}Pb$, $^{143}Nd/^{144}Nd$ and $^{176}Hf/^{177}Hf$ systematics (Blichert-Toft et al., 2005). This seems in agreement with the large offset (around 200 km) between the Kolbeinsey and Mohns Ridges, following the demonstration that transform faults reduce along-axis plume-driven flux in proportion to increasing transform offset length (Georgen and Lin, 2003).

A lateral deflection of the Iceland plume to distances of about 1000 km from Iceland, i.e. at least as far as to Jan

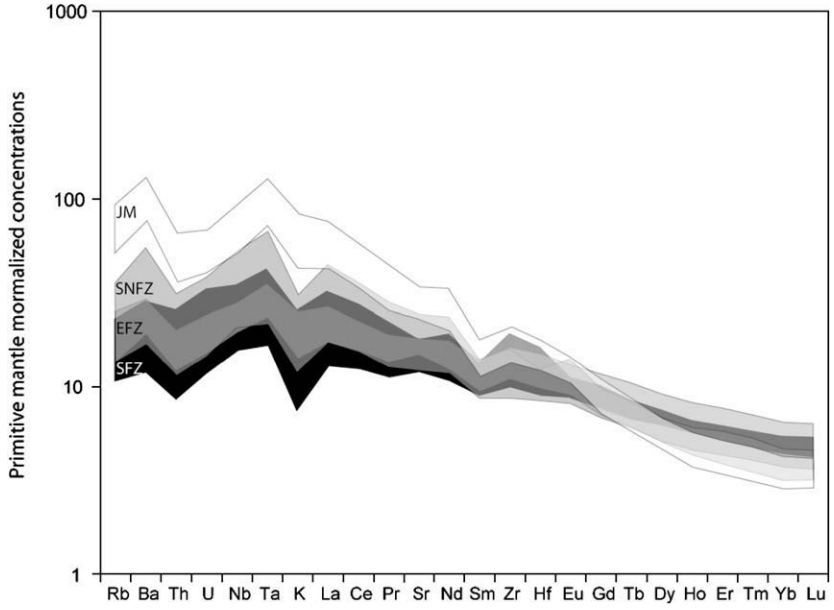

Fig. 5. Primitive mantle normalized incompatible trace element concentrations for (JM) Jan Mayen Island, (SNFZ) Snæfellness Volcanic Flank Zone, (EFZ) Eastern Volcanic Flank Zone, and (SFZ) Southern Volcanic Flank Zone. Primitive mantle concentrations from McDonough and Sun (1995).

Mayen Island, is supported by the presence of V-shaped ridges (Jones et al., 2002; Breivik et al., 2006). The shallow part of the lateral plume flow from Iceland is not preferentially channeled exactly beneath the ridges themselves but is sub-parallel to nearby oceanic spreading centers (Ito, 2001). Hot and fertile material from the Iceland plume could therefore migrate at depth along a path parallel to, but 200–300 km SE of, the Kolbeinsey Ridge towards Jan Mayen. In the direction of Jan Mayen, this laterally flowing mantle will not melt by decompression until it reaches the tensional setting near the southern tip of the Mohns Ridge. In this tensional environment, the fertile material may ascend, and undergo low-degree partial melting. This hypothesis is consistent with the present-day volcanic activity on Jan Mayen, as new and fertile material is still brought beneath the island. Further melting at gradually shallower levels continues along the Mohns Ridge north of the Jan Mayen Fracture Zone. In contrast, melting along the anomalously shallow Kolbeinsey Ridge is more extensive (Haase et al., 1996) and appears to have erased much of the Iceland mantle plume signature in that area (Trønnes et al., 1999).

5.3. Components existing in the Iceland mantle plume

The Os–Sr–Nd–He isotopes of the NE Atlantic basaltic suite (Fig. 4) suggests binary mixing relationships (hyperbolae) between two end-members with the Jan Mayen and Iceland flank zones basalts being at one extremity of the trend and Iceland rift zone basalts at the other. The additional information brought by Pb isotopes is discussed further in Section 5.5. The samples from Öræfajökull are considerably more radiogenic in their Sr-isotopic compositions and are clearly distinct from the pseudo-binary mixing trend (Fig. 4). The two main end-members are defined by their position at the extremities of the observed binary relationships and their possible meaning is discussed further. One, essentially observed in Jan Mayen basalts (JM end-member) and one, sampled in the Icelandic Rift Zone volcanics (IRZ end-member) have the following characteristics (Fig. 4):

JM end-member: high $^{87}Sr/^{86}Sr$ (~0.7035), low $^{143}Nd/^{144}Nd$ (~0.5129), low $^{187}Os/^{188}Os$ (~0.126), low $^{3}He/^{4}He$ (~6 Ra).

IRZ end-member: low $^{87}Sr/^{86}Sr$ (~0.7028), high $^{143}Nd/^{144}Nd$ (~0.5132), high $^{187}Os/^{188}Os$ (~0.136), high $^{3}He/^{4}He$ (~20 Ra) (Brandon et al., 2007).

It has been proposed that two end-members co-existing in the Iceland mantle plume could be the upper and lower sections of a recycled oceanic crust, basalts and gabbros, respectively (Chauvel and Hémond, 2000). According to this model, the alkaline lavas, more enriched in incompatible trace elements, would reflect the melting of the fertile basaltic portion of the oceanic crust, while the more depleted picrites and tholeiites are derived from more refractory gabbroic cumulates and suboceanic lithosphere. Using $^{187}Os/^{188}Os$ systematics, this hypothesis has already been successfully tested in Hawaii (Lassiter and Hauri, 1998) but also proposed for Iceland (Skovgaard et al., 2001). Although attractive, this model is difficult to reconcile with the negative trend observed between $^{87}Sr/^{86}Sr$ and $^{187}Os/^{188}Os$ or positive trend between $^{143}Nd/^{144}Nd$ and $^{187}Os/^{188}Os$ (Fig. 4a and b). The positive correlation between $^{143}Nd/^{144}Nd$ and $^{187}Os/^{188}Os$ observed in Iceland (also existing in previous data sets from Skovgaard et al. (2001) and Brandon et al. (2007)) is also inconsistent with such a model because if the high $^{87}Sr/^{86}Sr$, low $^{143}Nd/^{144}Nd$ end-member represents melt contributions from enriched basaltic crust, the Os isotopic composition is also expected to be highly radiogenic. Lassiter and Hauri (1998) observed a positive trend between $^{87}Sr/^{86}Sr$ and $^{187}Os/^{188}Os$ and a negative trend between $^{143}Nd/^{144}Nd$ and $^{187}Os/^{188}Os$ in Hawaiian basalts where such a model was advocated.

Different modes of enrichment may produce contrasting behaviors for lithophile isotopic systems, as represented by $^{87}Sr/^{86}Sr$ or $^{143}Nd/^{144}Nd$, and siderophile systems such as $^{187}Os/^{188}Os$. Although Hauri and Hart (1997) argued for an apparent missing high Re component, likely present in recycled ocean crust stored in the Earth's deep interior, Becker (2000) has shown that up to 60% of a slab's Re content can be lost during dehydration in subduction zones. Sun et al. (2003, 2004) also argued for a re-evaluation of the Re content of continental crust, which could be greater than previously estimated, due to Re transfer from slab to mantle wedge, and then to crust. Such a loss of Re from subducted oceanic crust would significantly modify the effect of addition of recycled oceanic crust to plume sources and consequently increase the amount of recycled crust or time necessary to generate high $^{187}Os/^{188}Os$ in OIB. The upper portion of the slab (i.e., the oceanic crust) would be more susceptible to Re-depletion than the lower gabbroic portion of the slab, generating lower Re/Os for the upper part and hence lower $^{187}Os/^{188}Os$. However, even a loss of 80% of Re can barely generate subchondritic $^{187}Os/^{188}Os$ ratios in 2 billion years (Ga) old oceanic crust. Consequently, the recycling of a whole section of an oceanic crust having an ITE-enriched basaltic crust, even variably depleted in Re, is unlikely to generate an end-member with subchondritic $^{187}Os/^{188}Os$.

The JM end-member requires enriched material, with a long time-integrated low Re/Os, low Sm/Nd and high Rb/Sr. The EM-1 like signature has been recognized in Iceland and was suggested to reside primarily in the shallow mantle beneath that region (Hanan and Schilling, 1997; Hanan et al., 2000; Blichert-Toft et al., 2005). The EM-1 signature observed at the Pitcairn hotspot, however, displays radiogenic $^{187}Os/^{188}Os$ (~0.15 (Eisele et al., 2002)) unlike material derived from the SCLM. The "C" component, defined by Hanan and Graham (1996) as mantle containing recycled ocean crust, is sometimes associated with high $^{3}He/^{4}He$ (deep) mantle. The "C" composition accounts for the moderately radiogenic Pb ($^{206}Pb/^{204}Pb = 19.6–20.0$) and $^{87}Sr/^{86}Sr$ (0.7035–0.7040) observed at many ocean islands, including Iceland. However, its composition is distinct from the low $^{3}He/^{4}He$ and $^{187}Os/^{188}Os$ values observed in this study, and by inference, recycled ocean crust is not the origin of the enriched component beneath Jan Mayen and Iceland.

Abyssal peridotites display $^{187}Os/^{188}Os$ values from very subchondritic to largely superchondritic values (~0.12–0.17) (Martin, 1991; Roy-Barman and Allègre, 1994; Snow

and Reisberg, 1995; Brandon et al., 2000; Alard et al., 2005; Harvey et al., 2006; Gannoun et al., 2007). Consequently, the subchondritic $^{187}Os/^{188}Os$ values observed in the JM end-member could simply reflect involvement of depleted upper mantle, as already proposed for the Gakkel Ridge, northward from Jan Mayen (Liu et al., 2008). However, abyssal peridotites show $^{87}Sr/^{86}Sr$ and $^{143}Nd/^{144}Nd$ very similar to MORB, corroborating the genetic relationship between them and a source depleted in ITE (e.g., Snow et al., 1994). In contrast, the JM end-member shows $^{87}Sr/^{86}Sr$ and $^{143}Nd/^{144}Nd$ typical for a source with long-term enrichment in ITE.

A subchondritic $^{187}Os/^{188}Os$ signature is also typical of subcontinental domains (e.g., Walker et al., 1989; Ellam et al., 1992). The Re–Os system is in most cases relatively insensitive to processes which enrich the subcontinental lithospheric mantle (SCLM) in incompatible trace elements (Ellam et al., 1992). Therefore, an ITE-enriched SCLM reservoir (e.g., McDonough, 1990) may preserve a history of low Re/Os expressed by subchondritic $^{187}Os/^{188}Os$ values (e.g., Walker et al., 1989). The presence of subcontinental domains dispersed in the upper mantle has been shown in several previous studies of OIB: Azores (Widom and Shirey, 1996), Kerguelen (Hassler and Shimizu, 1998; Ingle et al., 2002), possibly Austral-cook (Schiano et al., 2001), but also suspected along the Knipovich Ridge (Schilling et al., 1999), the Gakkel Ridge (Goldstein et al., 2008) and beneath Iceland (Hanan and Schilling, 1997). Alkali picrites erupted during early Tertiary rifting in West Greenland are also characterized by subchondritic $^{187}Os/^{188}Os$ ratios and have been ascribed to a SCLM source (Larsen et al., 2003). The presence of SCLM in the Iceland mantle plume could be related to the EM-1 like signature previously identified in Iceland (Hanan and Schilling, 1997; Schilling et al., 1999; Hanan et al., 2000; Blichert-Toft et al., 2005). The purported trace element and isotopic compositions of EM-1 mantle sources have been interpreted in terms of various components, including subducted pelagic sediments (Weaver, 1991; Chauvel et al., 1992; Rehkämper and Hofmann, 1997) and delaminated subcontinental lithospheric mantle (McKenzie and O'Nions, 1983; Mahoney et al., 1991; Hauri and Hart, 1993; Milner and LeRoex, 1996). The origin of such an EM-1 signature can be difficult to ascertain by lithophile isotope systems ($^{87}Sr/^{86}Sr$, $^{143}Nd/^{144}Nd$, $^{206,207,208}Pb/^{204}Pb$) but may be efficiently resolved by additional Os isotope data. The presence of pelagic sediments in the mantle source may explain the radiogenic Os isotope ratios observed in Pitcairn lavas (Eisele et al., 2002), whereas subchondritic Os isotope ratios in other EM-1 basalts can be related to subcontinental lithospheric mantle. The enriched EM-1 like end-member of the NE Atlantic mantle could thus be old and delaminated subcontinental mantle, dispersed in the convecting mantle and possibly also entrained by a rising plume (McKenzie and O'Nions, 1983). A similar explanation for the presence of subcontinental lithospheric mantle beneath the Kerguelen Island and in the Indian Ocean was suggested by Hassler and Shimizu (1998).

Whether this subcontinental material is an intrinsic part of the deep mantle plume or has been entrained in the plume during ascent through the uppermost mantle is still a matter of debate. The proximity to the Barents Sea-Svalbard continental platform and the combination of physical parameters like the northward decrease of spreading rates and partial melting degree have been used to explain the presence of entrained subcontinental lithospheric material along the Knipovich Ridge (Schilling et al., 1999), but also along the Gakkel Ridge (Goldstein et al., 2008). Finally, the systematic northward variations in trace elements concentrations and isotope ratios seem consistent with the pollution of the North Atlantic upper mantle with continental lithosphere during the rifting (Hanan et al., 2000). In any case, the higher temperature provided by the hot spot allows the SCLM to melt and contribute to the Iceland–Jan Mayen system isotopic signature.

An alternative explanation is a source involving old oceanic lithosphere. A recent study on Azores Islands lavas has suggested that old harzburgitic oceanic lithosphere is also characterized by $^{187}Os/^{188}Os$ subchondritic ratios (Schaefer et al., 2002). Subchondritic $^{187}Os/^{188}Os$ ratios have also been found in mantle xenoliths from Hawaii, far from any continental influence (Bizimis et al., 2007). It has already been proposed that both oceanic crust and oceanic lithosphere could be recycled at the same time (e.g., Moreira and Kurz, 2001; Bizimis et al., 2007). This model has also been successfully applied to the Hawaii mantle plume, by using $^{187}Os/^{188}Os$ ratios (Lassiter and Hauri, 1998). However, whereas Lassiter and Hauri (1998) observed a negative trend between $^{143}Nd/^{144}Nd$ and $^{187}Os/^{188}Os$ isotope ratios, samples from Iceland and Jan Mayen display a positive trend. Skovgaard et al. (2001) proposed that the low $^{187}Os/^{188}Os$ (0.127) observed in their IRZ picrite samples is related to the presence of depleted gabbros from the lower part of the oceanic crust and suboceanic lithosphere entrained in the Iceland mantle plume with $^{187}Os/^{188}Os$ values similar to abyssal peridotites (~0.124–0.126). However, as observed in the present data set, it would imply that the suboceanic lithosphere is also ITE-enriched, with higher $^{87}Sr/^{86}Sr$ and lower $^{143}Nd/^{144}Nd$. This is the opposite of what has generally been proposed for the enriched mantle source component(s) of oceanic mantle origin (Lassiter and Hauri, 1998; Chauvel and Hémond, 2000; Skovgaard et al., 2001).

On the other hand, the suboceanic lithosphere might be chemically similar to the subcontinental lithosphere if relatively analogous metasomatic processes occur in both. Although the suboceanic lithosphere is often involved in the genesis of OIB (e.g., Class and Goldstein, 1997; Lassiter and Hauri, 1998; Moreira and Kurz, 2001), subchondritic $^{187}Os/^{188}Os$-ratios have not previously been documented in oceanic basalts other than the Azores (Widom and Shirey, 1996; Schaefer et al., 2002). This may either imply that suboceanic lithosphere with subchondritic $^{187}Os/^{188}Os$ ratios is usually not sampled at oceanic islands except as mantle xenoliths (Bizimis et al., 2007) or that the suboceanic lithosphere does not develop subchondritic $^{187}Os/^{188}Os$ ratios. The tectonic setting has often been invoked to infer if the subchondritic $^{187}Os/^{188}Os$ ratios observed in OIB were related to the presence of subcontinental or suboceanic lithosphere (e.g., Hassler and Shimizu, 1998; Schaefer

et al., 2002; Bizimis et al., 2007). In the case of Iceland and more particularly of Jan Mayen, the young age of the opening of the North Atlantic ocean (~60 Ma ago) and the proximity of the continental margin make the subcontinental lithospheric mantle an especially appropriate candidate for the subchondritic $^{187}Os/^{188}Os$ ratios observed in Iceland and Jan Mayen.

In contrast to the ITE-enriched off-rift basalts, the olivine tholeiites and picrites from the rift zones are characterized by low $^{87}Sr/^{86}Sr$ and high $^{143}Nd/^{144}Nd$, $^{3}He/^{4}He$ and $^{187}Os/^{188}Os$ ratios. Because no mantle component displaying the latter combination of relative isotope ratios is known, mixing between several components is strongly favored. Elevated $^{187}Os/^{188}Os$ ratios in OIB have generally been interpreted as oceanic crust recycling (e.g., Reisberg et al., 1991; Roy-Barman and Allègre, 1995; Shirey and Walker, 1998), but this component is unlikely characterized by low $^{87}Sr/^{86}Sr$ and high $^{143}Nd/^{144}Nd$ and $^{3}He/^{4}He$. Traditionally, high $^{3}He/^{4}He$ ratios have been ascribed to primordial, undegassed material from the lower mantle. Some recent studies, however, have emphasized the fact that in OIB, the highest $^{3}He/^{4}He$-ratios often occur in highly refractory basalts and picrites with the highest $^{143}Nd/^{144}Nd$ and Mg-numbers and the lowest $^{87}Sr/^{86}Sr$ and ITE contents (e.g., Coltice and Ricard, 1999; Ellam and Stuart, 2004; Class and Goldstein, 2005; Albarède, 2008). Moreover, an experimental study of olivine-melt partitioning by Parman et al. (2005) indicates that U and Th are more incompatible in mantle residues than He. Strongly depleted mantle residues that formed early in the Earth's history may therefore be suitable candidates for the high $^{3}He/^{4}He$ source components in the mantle.

There is ample evidence that much of the Earth's mantle has been strongly melt-depleted in repeated events, largely associated with the major orogenic episodes. Some recent assessments of the $^{142}Nd/^{144}Nd$ chondritic value have discussed whether most of the mantle was originally depleted within the first 500 Ma (Boyet and Carlson, 2005, 2006). Material with high $^{3}He/^{4}He$ and $^{143}Nd/^{144}Nd$ and low $^{87}Sr/^{86}Sr$ could be derived from a depleted and isolated portion of the lower mantle. This model is in agreement with a recent study of Porcelli and Elliot (2008), indicating that a large depletion event that occurred >3 Ga ago better explains the unradiogenic He values in OIB compared to a continuous depletion of the mantle (Class and Goldstein, 2005). It thus seems reasonable to infer that this depleted mantle, distinct from the depleted-MORB mantle, is actually a part of the lower mantle. A model invoking partial isolation of deep mantle ITE-depleted, high $^{3}He/^{4}He$ reservoir offers several advantages. It is easier to keep such reservoirs isolated over relatively long time periods in a highly viscous lower mantle, especially if primordial He resides in refractory cumulates (Albarède, 2008). The long-term storage of a relatively undegassed source away from the upper mantle melting regions is required to explain the close-to-solar-values neon isotope ratios measured in Icelandic lavas (Dixon et al., 2000; Moreira et al., 2001; Dixon, 2003). Recycled oceanic crust located at the bottom of the mantle is likely to be negatively buoyant. Assuming that the Iceland mantle plume originated in the lower mantle, possibly at the core–mantle boundary (Helmberger et al., 1998; Bijwaard and Spakman, 1999; Shen et al., 2002; Li et al., 2003; Zhao, 2004; Montelli et al., 2006), mixture of recycled oceanic crust with another deep and likely peridotitic component is required in order for the plume to rise (Niu and O'Hara, 2003; Sobolev et al., 2007).

Some Iceland samples show $^{87}Sr/^{86}Sr$, $^{143}Nd/^{144}Nd$ and $^{206,207,208}Pb/^{204}Pb$ values that are very depleted (e.g., Thirlwall et al., 2004) and close to the values inferred for the DMM (see compilation in Workman and Hart (2005)). DMM material is hence likely involved in Iceland magmatism because it would otherwise imply that a component present in the Iceland plume would be even more depleted than the DMM. Involvement of DMM is in agreement with the model of Hauri et al. (1994) showing the entrainment of material surrounding the plume conduit due to heat diffusion. The contribution of DMM material in the Iceland mantle plume is corroborated by numerous studies (Mertz et al., 1991; Haase et al., 1996; Hanan and Schilling, 1997; Dixon et al., 2000; Hanan et al., 2000; Dixon, 2003; Stracke et al., 2003; Blichert-Toft et al., 2005) though several authors argued against the presence of DMM material in lavas erupted in Iceland (Fitton et al., 1997; Chauvel and Hémond, 2000; Kempton et al., 2000; Skovgaard et al., 2001; Fitton et al., 2003; Kokfelt et al., 2006; Thirlwall et al., 2006). Skovgaard et al. (2001) acknowledged that the near-chondritic $^{187}Os/^{188}Os$ values observed in picrites are close to the DMM values, but they attributed the low $\delta^{18}O$ of the same samples to the presence of hydrothermally altered suboceanic lithosphere in their source. Although the model developed here includes a large portion of DMM material in the Iceland and Jan Mayen lavas, the $^{187}Os/^{188}Os$ ratios cannot actually clarify this issue, but exclude a large role of recycled oceanic gabbro cumulates and suboceanic lithosphere (Chauvel and Hémond, 2000; Skovgaard et al., 2001; Kokfelt et al., 2006) in the JM end-member. One can argue that the geochemically DMM-like depleted signal observed in the IRZ mixture is due to recycled suboceanic lithosphere, but then, it would mean that old suboceanic lithosphere recycled with the oceanic crust has a present-day isotope signature similar to the current asthenosphere under Iceland. While this hypothesis is possible, a simpler explanation favors that the depleted component is derived from entrainment of the local depleted asthenosphere in the source mixture.

The involvement of at least 4 components in the NE Atlantic mantle can be reconciled with the observation of binary correlations by applying the systematics of "pseudo-binary mixing" (Hanan et al., 1986; Schilling et al., 1992; Douglass and Schilling, 2000; Debaille et al., 2006a). The two main (final) end-members can be generated by progressively reducing the number of initial components by successive mixing steps likely separated in space and time. The pseudo-binary mixing of 4 major components is not in contradiction with the several end-members defined in $^{206,207,208}Pb/^{204}Pb$ space (Thirlwall et al., 2004). The goal of the pseudo-binary mixing systematic is only to reconcile the observed, mostly binary, co-variations with the involvement of several end-members in the mixing. The

Öræfajökull basalts seem to sample an additional fifth mantle source component that is clearly unique to this volcanic system (Prestvik et al., 2001; Kokfelt et al., 2006). Consequently, this component is not included in the following, but its existence is not in contradiction with the model presented here (Fig. 6c).

5.4. Model of the pseudo-binary mixing

In a multistage mixing context, the NE Atlantic mantle sources have been modeled using four primary components. A series of models, using slightly variable element abundances and isotopic compositions, were tested. Fig. 6 and Table 5 represent the model that seems most consistent with the geochemical and geological evidence. However, it is important to keep in mind that the solution is not unique, except for the involvement of SCLM, which is required by the $^{187}Os/^{188}Os$ systematics of Iceland and Jan Mayen samples. The four primary components are:

(1) Recycled oceanic crust with minor amounts (1.5%) of sediments (ROC). Kokfelt et al. (2006) and Brandon et al. (2007) modeled a 1–2 Ga recycled oceanic crust in the source of Iceland plume. An age of 1 Ga has been used here. However, this age is model-dependant and is consequently not constrained by the present model. The quantitative recycling model proposed by Stracke et al. (2003) has been applied in order to determine the isotopic compositions and trace elements concentrations of a 1 Ga recycled oceanic crust. This component has the highest $^{187}Os/^{188}Os$ ratio of 7.3 and $^{87}Sr/^{86}Sr$, $^{143}Nd/^{144}Nd$ and $^{3}He/^{4}He$ (R/Ra) of 0.703544, 0.513011 and 7, respectively (Hanyu and Kaneoka, 1997; Graham et al., 1998; Stracke et al., 2003; Brandon et al., 2007).

(2) Depleted lower mantle (DLM) formed by ancient melt extraction but still displaying a primordial $^{3}He/^{4}He$ signature (Porcelli and Elliot, 2008). An intermediate value for Sr and Nd isotopic composition and ITE concentrations has been arbitrarily fixed as a mixture of 20% DMM (values as in Table 5) and 80% BSE. This corresponds to $^{87}Sr/^{86}Sr = 0.703852$ and $^{143}Nd/^{144}Nd = 0.512874$. The BSE ITE concentrations are from McDonough and Sun (1995) and $^{87}Sr/^{86}Sr = 0.7045$ and $^{143}Nd/^{144}Nd = 0.512638$. The DLM ITE concentrations are listed in Table 5. The $^{187}Os/^{188}Os$ (0.1296) and Os concentration of the primitive upper mantle (PUM) is used (Meisel et al., 2001). The

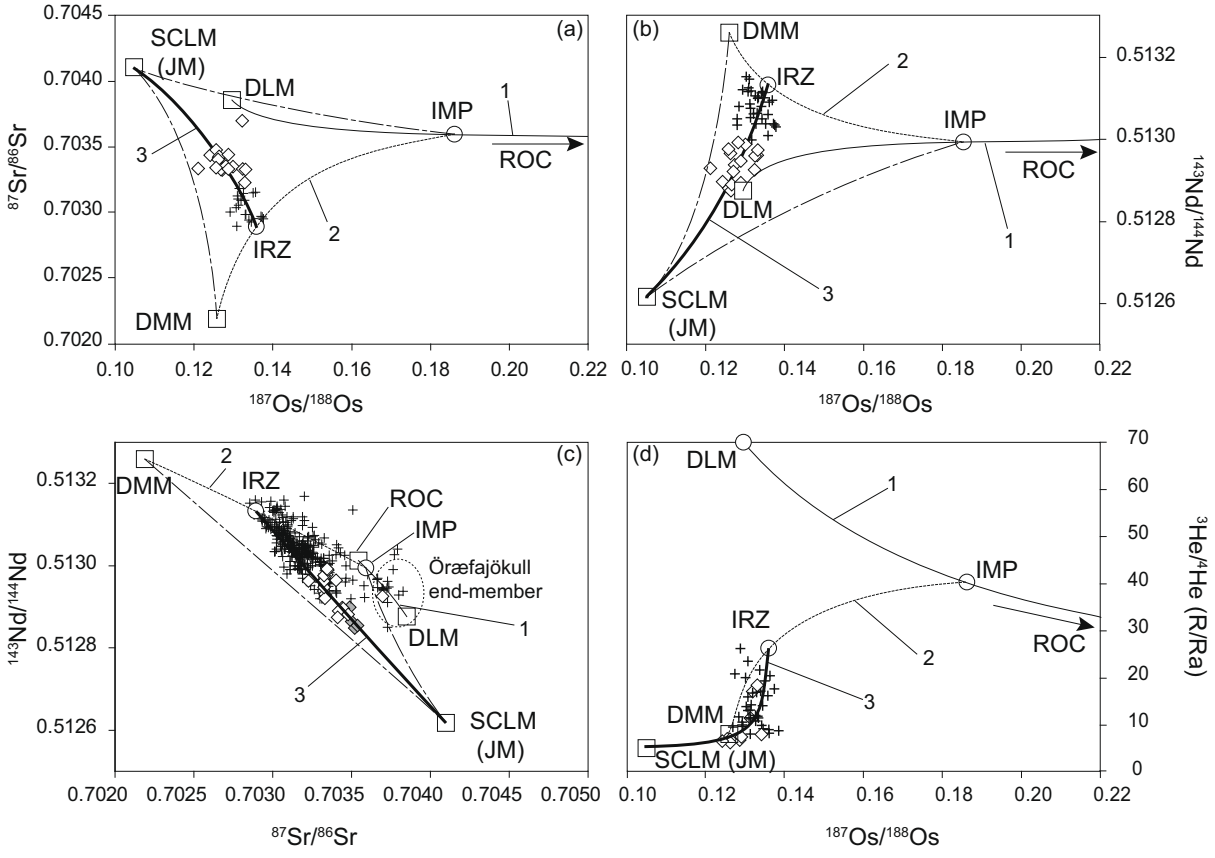

Fig. 6. (a) $^{143}Nd/^{144}Nd$ vs. $^{87}Sr/^{86}Sr$, (b) $^{143}Nd/^{144}Nd$ vs. $^{187}Os/^{188}Os$, (c) $^{87}Sr/^{86}Sr$ vs. $^{187}Os/^{188}Os$, and (d) $^{3}He/^{4}He$ (R/Ra) vs. $^{187}Os/^{188}Os$ diagrams presenting the pseudo-binary mixing model used to model the Iceland and Jan Mayen data. The different mixing steps between the different components in order to explain the binary mixing observed in Iceland are showed by number 1, 2 and 3. Step 1 (plain line): mixing between the depleted lower mantle (DLM) and the recycled oceanic crust (ROC), in order to generate the signature of the Iceland mantle plume (IMP). Step 2 (small dashed line): mixing between the IMP and the depleted-MORB mantle (DMM), in order to generate the IRZ end-member. Step 3 (bold line): mixing between IRZ, and the subcontinental lithospheric mantle (SCLM, JM), likely present as fragments dispersed in the upper mantle. Diamond: this study; cross: literature data (as in Fig. 4).

Table 5
Concentrations and isotopic compositions of the components used in the model.

	ROC Slab 1 Ga + 1.5%sed	DLM	IMP ROC+DLM	DMM	IRZ IMP+DMM	SCLM	E1 DMM+SCLM	E2 DMM+SCLM
$^{187}Os/^{188}Os$	7.34589[a]	0.12960[d]	0.18617	0.12600[h]	0.13596	0.10500[l]	0.11705	0.12467
$^{87}Sr/^{86}Sr$	0.703544[b]	0.703852[e]	0.703592	0.70219[i]	0.702891	0.704100[m]	0.703496	0.702504
$^{143}Nd/^{144}Nd$	0.513011[b]	0.512874[e]	0.512993	0.51326[i]	0.513132	0.512617[m]	0.512819	0.513154
$^{3}He/^{4}He$ (R/Ra)	7[c]	70[f]	40.20	8[j]	25.78	5[n]	5.12	5.93
$^{206}Pb/^{204}Pb$			19.8[g]	17.573[i]	19.577	18.500	18.310	17.814
$^{207}Pb/^{204}Pb$			15.59[g]	15.404[i]	15.571	15.420	15.417	15.408
$^{208}Pb/^{204}Pb$			39.45[g]	37.000	39.205	38.400	38.113	37.364
[Os]	0.00008[a]	0.003[d]	0.00198	0.0033[a]	0.00297	0.002[o]	0.00259	0.00317
[Sr]	82.0[b]	8.1[e]	33.9	11.3[k]	17.0	20[p]	16.1	12.2
[Nd]	7.66[b]	0.62[e]	3.09	1.12[k]	1.61	2[p]	1.60	1.21
He*	5	3	3.7	1	1.7	20	11.5	2.9
[Pb]	0.35[b]	1.93[e]	1.38	0.05[k]	0.38	0.16[p]	0.11	0.06
			ROC		IMP		DMM	DMM
		Mixing proportion	35%		25%		45%	90%

ROC, recycled oceanic crust; DLM, depleted lower mantle; IMP, Iceland mantle plume; DMM, depleted-MORB mantle; SCLM, subcontinental lithospheric mantle; IRZ, Iceland rift zone end-member; E1 and E2, end-members 1 and 2 resulting from the mixture of DMM and SCLM (see text for detail). Mixing proportions of one component in each mixture are indicated. Os, Sr and Nd concentrations in ppm.
(a) Brandon et al. (2007); (b) Stracke et al. (2003); (c) (Hanyu and Kaneoka (1997); (d) Meisel et al. (2001); (e) DLM modeled as a mixture of 20% DMM and 80% BSE, DMM as in Table 5, BSE trace element concentrations from McDonough and Sun (1995) (see text for details); (f) adapted from Ellam and Stuart (2004); (g) Hanan and Schilling (1997); (h) Gannoun et al. (2007); (i) Workman and Hart (2005); (j) Farley and Neroda (1998); (k) Rehkämper and Hofmann (1997); (l) Ellam et al. (1992); (m) Lee et al. (1994); (n) Gautheron and Moreira (2002); (o) Lee and Walker (2006); (p) McDonough (1990).
* Concentrations in He expressed in relative value between each component, see text for more details.

$^{3}He/^{4}He$ (Ra) value of DLM is estimated at 70 times the atmospheric ratio, somewhat higher than the value of 60 proposed by Ellam and Stuart (2004).

(3) Depleted asthenospheric MORB-mantle (DMM), formed by semi-continuous and therefore relatively recent melt extraction associated with oceanic crust formation. The DMM reservoir, located in the upper mantle, has evolved by successive melt enrichment and depletion processes over much of Earth's history. The $^{87}Sr/^{86}Sr$ and $^{143}Nd/^{144}Nd$ value have been chosen from the depleted-MORB-source of Workman and Hart (2005), in order to take into account the very depleted $^{87}Sr/^{86}Sr$ and $^{143}Nd/^{144}Nd$ signatures observed in Iceland. The Sr and Nd concentrations are from Rehkämper and Hofmann (1997). The $^{187}Os/^{188}Os$ composition of the DMM (0.126) is taken from the average value of MORB Os-rich sulphide (Gannoun et al., 2007). The average $^{3}He/^{4}He$-ratio of DMM is 8 times the atmospheric ratio (Farley and Neroda, 1998).

(4) Subcontinental lithospheric mantle (SCLM) affected by strong melt depletion (Re-loss), followed by enrichment events. The SCLM component has the lowest $^{187}Os/^{188}Os$ ratio of 0.105 and $^{87}Sr/^{86}Sr$, $^{143}Nd/^{144}Nd$ and $^{3}He/^{4}He$ of 0.7041, 0.5126 and 5, respectively. The SCLM composition is based on Ellam et al. (1992) for $^{187}Os/^{188}Os$, and from a harzburgitic sample from the Cameroon line for $^{87}Sr/^{86}Sr$ and $^{143}Nd/^{144}Nd$ compositions (Lee et al., 1994). It is difficult to determine an average concentration for the SCLM, because of the very large variation range observed in xenoliths, but this choice will only influence the mixing proportion of this model and not the general pattern of the pseudo-binary mixing systematic. It has recently been proposed that the SCLM could be less depleted in Os than previous estimates (0.2 ppb (Ellam et al., 1992)), with an Os concentration around 2–3 ppb (Pearson et al., 1995; Lee and Walker, 2006). The latter value has been used in the model. For Sr and Nd concentrations, SCLM median values proposed by McDonough (1990) have been used. The $^{3}He/^{4}He$ (R/Ra) has been chosen in the range measured by Gautheron and Moreira (2002).

The He concentrations in these four components have been estimated and expressed in relative proportions. The He content of the DMM and the DLM has been arbitrarily fixed at 1 and 3, respectively, since the DLM has also been depleted, but less than the DMM. The He content of old oceanic crust is a balance between He loss at mid-oceanic ridges and subduction zones, and He production from Th and U radioactive disintegration with time. This value has been adapted from Brandon et al. (2007), and fixed at 5. The high He content of the SCLM (20) also reflects the production of radiogenic He due to the high content in radioactive trace elements (Gautheron and Moreira, 2002).

The Iceland mantle plume (IMP) is modeled as a first-stage mixture of 35% ROC and 65% DLM. It has previously been proposed that the plume has a composition similar to the "C" component (Hanan and Schilling, 1997), and the result of this initial mixing reproduces approximately the Sr–Nd isotopic compositions of "C". The IMP $^{3}He/^{4}He$ resulting from this mixing is ~40, a value comparable to that measured in Baffin Island samples (up to 50), representing the proto-Iceland mantle plume (Stuart et al., 2003). It is important to note that at this point, the mixture between the DLM and ROC is considered as homogeneous, and that the IMP is consequently a component by itself.

The IRZ end-member, relatively depleted in lithophile elements, is modeled as a second-stage mixture of 25% IMP and 75% DMM during the ascent of the plume in the upper mantle. These proportions finally result in ~9% of recycled oceanic crust material in melts beneath Iceland, close to the 10% of recycled oceanic crust in the Iceland mantle plume proposed by Sobolev et al. (2007). Such proportions of depleted mantle in the melting zone under Iceland may be explained by the presence of the Mid-Atlantic Ridge and the simultaneous generation of MORB. There are other examples of the partial involvement of DMM-sources in OIB volcanism. White et al. (1993) demonstrated a concentric isotope pattern in the Galapagos area and attributed this to the entrainment of surrounding MORB mantle by the ascending plume. The magnitude of the depleted signature from the DMM is probably linked to the location of the Iceland plume close to the NE Atlantic plate boundary, favoring mixing between ascending plume material and the shallow asthenosphere; but also to the fact that the mantle plume could represent a rising chain of blobs instead of a continuous column (Schilling and Noe-Nygaard, 1974; Montelli et al., 2006), implying that the upper mantle is not continuously polluted by the mantle plume.

The main binary mixing trends observed in Fig. 6 are governed by the third-stage IRZ versus the SCLM (JM) end-members. However, this mixing is incomplete, as seen by the dispersion around the main mixing hyperbola (especially in the $^{87}Sr/^{86}Sr$ and $^{143}Nd/^{144}Nd$ diagram, Fig. 6c). The dispersion likely indicates variable proportions and imperfect mixing of the different end-members at small-scale. The high $^{87}Sr/^{86}Sr$ samples from Öræfajökull area fall on the mixing line between ROC and DLM (Fig. 6c). But since the value of the DLM have been fixed arbitrarily, it is difficult to draw any conclusion. Additional small heterogeneity beyond the 4 original components defined in Sr–Nd–Os–He isotope space may also contribute to the dispersion (Thirlwall et al., 2004).

The two ITE-enriched SCLM and IMP components differ mainly by their distinct $^{187}Os/^{188}Os$, but also by the lower $^{143}Nd/^{144}Nd$ and $^{3}He/^{4}He$ and higher $^{87}Sr/^{86}Sr$, of the SCLM. Whether the subcontinental lithospheric mantle (JM end-member) was entrained in and mixed with the mantle plume material in the lower mantle, possibly well before the ascent of the plume, is still uncertain. It is possible that the SCLM, as well as the DMM, reside in the upper mantle before entrainment in the ascending, and possibly partially molten, mantle source (Goldstein et al., 2008). The common geochemical features throughout Iceland, Jan Mayen and the Reykjanes, Kolbeinsey and Mohns spreading ridges may support this scenario (Schilling et al., 1999; Hanan et al., 2000). The southwards decreasing SCLM signal (from Jan Mayen to Iceland) can be explained by variable proportions of SCLM within the upper mantle, but also by variable degrees of partial melting (increasing southwards), resulting in larger dilution of the same amount of enriched material by the surrounding depleted mantle. The complexity of the Iceland–Jan Mayen system is related not only to source variations, but also to dynamic and progressive melting of these sources.

5.5. The lead perspective

While Iceland rift zones, volcanic flank zones and Jan Mayen samples show binary relationships in $^{143}Nd/^{144}Nd$ and $^{87}Sr/^{86}Sr$ vs. $^{187}Os/^{188}Os$ diagrams, but also in $^{206}Pb/^{204}Pb$, $^{207}Pb/^{204}Pb$ and $^{208}Pb/^{204}Pb$ space, $^{87}Sr/^{86}Sr$ vs. $^{206}Pb/^{204}Pb$ diagram do not provide such binary alignment (Fig. 7). The main reason is that Jan Mayen samples do not define an extreme end-member in the Pb isotopic space (Trønnes et al., 1999), on the contrary of what is observed in the Os–He–Nd–Sr space. Because Jan Mayen samples, using $^{187}Os/^{188}Os$, have been shown displaying the greatest proportion of SCLM in their source, the Pb isotopic composition of SCLM is inferred to be in the direction of, but beyond the Jan Mayen cluster. This results in an intermediate $^{206}Pb/^{204}Pb$ (18.5) and $^{208}Pb/^{204}Pb$ (38.4) but low $^{207}Pb/^{204}Pb$ (15.42) component. This is in contradiction with the use of an EM-1 composition as proposed by Hanan and Schilling (1997) because EM-1 component has a too low $^{206}Pb/^{204}Pb$ (16.5) and too high $^{207}Pb/^{204}Pb$ (15.85) values that are not reconcilable with Jan Mayen data. Interestingly, the prevalence of a low $^{207}Pb/^{204}Pb$ (and low $^{207}Pb/^{206}Pb$) component under Iceland has been noted in previous studies (Thirlwall, 1995; Stracke et al., 2003). Using the composition of the SCLM component just defined with Jan Mayen basalts, the low $^{207}Pb/^{204}Pb$ in most of the Icelandic VFZ basalts may be ascribed to the SCLM component.

As the SCLM Pb isotopic composition is intermediate between DMM and IMP, binary relationships are not observed when Pb isotopes are included. On the other hand, as an illustration that the model previously proposed, where the IMP mixes with DMM and then with SCLM, is not unique, a second mixing model can be developed using the three previously defined components (DMM, SCLM, IMP) (Fig. 7). The Pb values used in both the first and the second models are presented in Table 5, and are from Hanan and Schilling (1997) for the IMP, and from Workman and Hart (2005) for DMM. In the second model, the DMM is variably polluted by SCLM before mixing with the IMP, resulting in two end-members: E1 (45% DMM, 55% SCLM), and E2 (90% DMM, 10% SCLM). Graphically, this second model is also very satisfying, included the dispersion existing in the $^{3}He/^{4}He$ vs. $^{187}Os/^{188}Os$ diagram (Fig. 7f). The Pb systematics (Fig. 7a and b) is better explained by the second model. The first model (IMP mixes with DMM, and then with SCLM) better explains the main trend in $^{143}Nd/^{144}Nd$ vs. $^{87}Sr/^{86}Sr$, and $^{143}Nd/^{144}Nd$ and $^{87}Sr/^{86}Sr$ vs. $^{187}Os/^{188}Os$ diagrams, and the high $^{3}He/^{4}He$ values in IRZ samples, but the second model (IMP mixes with DMM+SCLM) reproduces the two clusters (Iceland rift zones; and Iceland volcanic flank zone and Jan Mayen samples) that are observed (Fig. 7e). In addition, the two models provide mixing directions that are roughly orthogonal, resulting in several different end-members (e.g., IRZ, E1, E2) that add geochemical complexity in the Iceland–Jan Mayen system.

In order to recognize the different information provided by the Pb isotopic systems, a principal component analysis (PCA) has been realized on several datasets. It has been

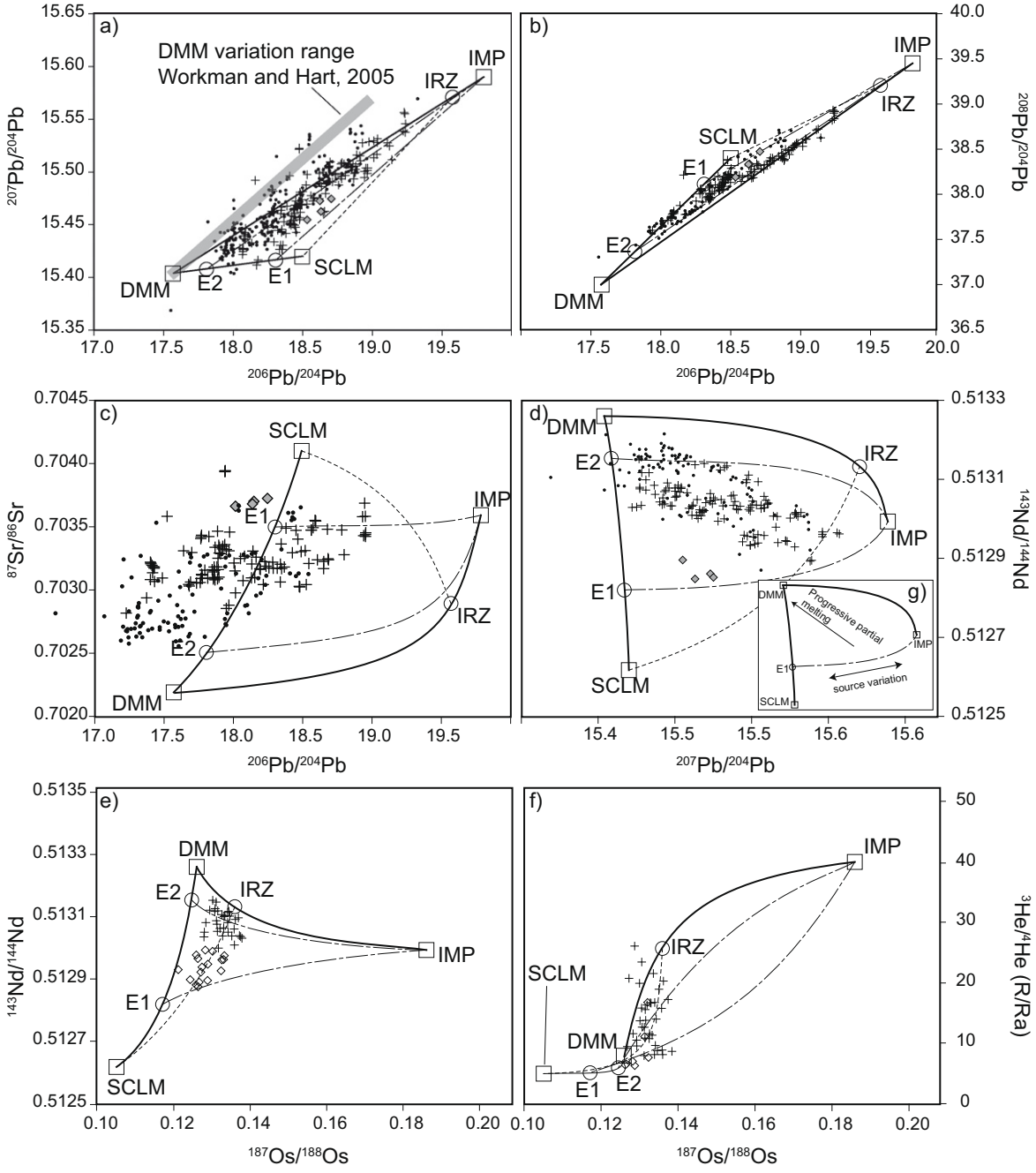

Fig. 7. (a) $^{207}Pb/^{204}Pb$ vs. $^{206}Pb/^{204}Pb$, (b) $^{208}Pb/^{204}Pb$ vs. $^{206}Pb/^{204}Pb$, (c) $^{87}Sr/^{86}Sr$ vs. $^{206}Pb/^{204}Pb$, (d) $^{143}Nd/^{144}Nd$ vs. $^{207}Pb/^{204}Pb$, (e) $^{143}Nd/^{144}Nd$ vs. $^{187}Os/^{188}Os$, (f) $^{3}He/^{4}He$ (R/Ra) vs. $^{187}Os/^{188}Os$ diagrams presenting the two mixing models accounting for the geochemical variation in the Iceland–Jan Mayen system. Both models include several mixing steps, separated in space and time. In the first model, step 1: ROC+DLM = IMP (not shown, see Fig. 6), step 2: IMP+DMM = IRZ, step 3: IRZ+SCLM; in the second model, step 1: ROC+DLM = IMP (as in the first model), step 2: DMM+SCLM = E1 and E2 (depending of variable amounts of SCLM (Fig. 7e), or variable degrees of partial melting of the DMM (Fig. 7g)), step 3: IMP+E1, and IMP+E2. Same symbols as in Fig. 6. Literature Pb data from Schilling et al. (1999), Trønnes et al. (1999), Thirlwall et al. (2004), Blichert-Toft et al. (2005), Kokfelt et al. (2006).

shown that performing a PCA on multiple isotopic systems may introduce fake end-members because mixing lines between the end-members are non-linear (Blichert-Toft et al., 2005; Debaille et al., 2006b). Consequently, PCA using only Pb isotopes may be helpful. Two different datasets have been used, one for North Atlantic MORB samples (Schilling et al., 1999; Thirlwall et al., 2004; Blichert-Toft et al., 2005), and one for Iceland and Jan Mayen Islands (Trønnes et al., 1999; Thirlwall et al., 2004; Kokfelt et al., 2006). As already demonstrated by Blichert-Toft et al. (2005), the PCA using Pb isotopes on North Atlantic MORB samples reveals only two principal components

(i.e., three end-members) accounting for 98.40% and 1.52% of the variance. Interestingly the PCA on Iceland and Jan Mayen samples (Trønnes et al., 1999; Thirlwall et al., 2004; Kokfelt et al., 2006) unravels three principal components (i.e., four end-members), accounting for 92.97%, 5.78% and 1.25% of the variance. The last principal component displays a very weak signal, likely highlighting the small Öræfajökull end-member that may reflect the mixture between ROC and DLM (Fig. 6c). This result implies that, except for this last minor component, only three components are required to generate the isotopic variations in North Atlantic MORB and Iceland. Any other end-member can be explained by the mixture between the three components, or alternatively by variables degrees of partial melting between the components. For example, E2 can also reflect an increasing degree of partial melting of the upper mantle. In this case, magma sources lie on the E1-IMP mixing curve, but are progressively diluted towards more depleted compositions, because of a greater participation of the depleted upper mantle consecutive to higher degrees of partial melting (Fig. 7g). Consequently, the greater SCLM geochemical signal in Jan Mayen lavas could simply reflect a smaller contribution of the DMM because of smaller degrees of partial melting, instead of a greater proportion of SCLM.

Finally, both models are able to take into account the range in isotopic variation of the North Atlantic system. The IMP enters in the upper mantle and entrains depleted material. The ascent column is relatively homogenized at this level, generating the IRZ end-member. Progressively, at shallower depth, the remaining IMP mixes with DMM polluted by small amount of refractory SCLM (E1 and E2 end-members). Larger blobs of SCLM, requiring heat from the IMP in order to melt, are also expected. This complexity is likely related to the interaction between the mantle plume and the mid-oceanic ridge, the presence of disseminated SCLM fragments but also to the fact that the Iceland plume is not continuous (Montelli et al., 2006). The several end-members possibly identified within the Iceland mantle plume (e.g., Thirlwall et al., 2004) may reflect different levels of mixing in the mantle, different proportions of components, but also variable degrees of partial melting of the primary components.

6. CONCLUSION

Multi-isotopic analysis of lavas from Jan Mayen and Iceland's volcanic flank zones reveal a genetic relationship in their origin. The $^{187}Os/^{188}Os$ ratios of these enriched basalts are lower than for all other OIB suites except the Azores. The lack of correlation between Re/Os and $^{187}Os/^{188}Os$ indicates that the $^{187}Os/^{188}Os$ ratios are not influenced by assimilation of crustal material during fractional crystallization processes. Discrepancies between pure olivine and whole rock powders indicate that $^{187}Os/^{188}Os$ ratios were not influenced by shallow contamination processes (sediments, sea water) for lavas with Os contents higher than 30 ppt. Co-variations are observed between $^{187}Os/^{188}Os$, $^{143}Nd/^{144}Nd$, $^{87}Sr/^{86}Sr$ and $^{3}He/^{4}He$ in lavas from Jan Mayen and Iceland. The most enriched mantle source end-member of the NE Atlantic is sampled preferentially by the strongly alkaline Jan Mayen basalts, and it has low $^{187}Os/^{188}Os$ combined with low $^{143}Nd/^{144}Nd$ and $^{3}He/^{4}He$ and high $^{87}Sr/^{86}Sr$. The weakly alkaline to tholeiitic basalts of the Icelandic volcanic flank zones have compositional ranges overlapping with and intermediate between the Jan Mayen basalts and the olivine tholeiites and picrites of the Icelandic rift zones and the nearby spreading ridge segments. The depleted end-member, preferentially sampled in Iceland rift zones, has higher $^{187}Os/^{188}Os$, $^{143}Nd/^{144}Nd$ and $^{3}He/^{4}He$ and lower $^{87}Sr/^{86}Sr$. The geochemical similarities between Iceland volcanic flank zones and Jan Mayen samples strongly support a genetic relationship between Jan Mayen Island and the Iceland mantle plume. The tensional environment of Jan Mayen Island, near the Jan Mayen Fracture Zone and the southern tip of the Mohns Ridge, can explain the ascent and the low-degree partial melting of fertile material from the Iceland mantle plume flowing northeastwards.

Multi-element isotopic modeling of the relative contribution from various mantle source components requires at least 3 components (IMP (modeled as a mixture of DLM and ROC), DMM, and SCLM). The positive correlation between $^{187}Os/^{188}Os$ and $^{143}Nd/^{144}Nd$ ratios suggests that the Jan Mayen end-member, with subchondritic $^{187}Os/^{188}Os$, is sampling a subcontinental lithospheric mantle component (SCLM). This old source was presumably subjected to ancient melt depletion, followed by later metasomatic events that led to Rb/Sr, Nd/Sm and U/He enrichment but preserved low Re/Os. While this SCLM component might have been incorporated into the Iceland plume at a deep level, it may have more likely been dispersed in the uppermost mantle during opening of the North Atlantic Ocean. Although refractory, SCLM can melt in this region because of the heat provided by the Iceland hot spot. The second end-member, with high $^{187}Os/^{188}Os$, $^{143}Nd/^{144}Nd$ and $^{3}He/^{4}He$ and low $^{87}Sr/^{86}Sr$ is the result of the mixing between several components, two depleted (depleted lower mantle and depleted-MORB mantle) and one enriched (recycled oceanic crust). Although this model, where the IMP mixes with the DMM and then with the SCLM, is non-unique, a PCA using Pb isotopes clearly indicates that all the variability encountered in the Iceland–Jan Mayen system can be described with only 3 principal components. In order to satisfy the Pb systematics, a second model, where the DMM mixes first with variable amount of SCLM, before mixing with the IMP can also be developed using the same parameters from the first model. It is possible that both these models occur, adding several end-members and consequent complexity in the Iceland–Jan Mayen system.

ACKNOWLEDGMENTS

This work was supported by a postdoctoral fellowship grant to V.D. at the Lunar and Planetary Institute, NSF Grants EAR0000908 to A.D.B. and OCE 0241915 to D.W.G. The field and analytical work at NVC, Reykjavik was covered by a grant to R.G.T. from RANNIS. A. Agranier is thanked for his analytical support during PGE measurements on the ICP-MS Thermofinni-

Table A1
Trace elements concentrations for whole-rocks, olivine enriched whole-rocks, olivines and percentage enrichment.

	Normal whole-rocks									Olivine enriched whole-rocks								
	JAN 23	JAN 246	SNS 201	SNS 209	SNS 214	HAIN	SAL 690	SAL 768	NAL 759	JAN 23	JAN 246	SNS 201	SNS 209	SNS 214	HAIN	SAL 690	SAL 768	NAL 759
Rb	32.3	31.8	8.1	15.8	21.1	13.7	9.9	8.2	15.1	14.9	12.4	6.1	7.1	14.8	7.7	10.0	2.8	11.6
Ba	537	541	110	219	346	187	118	127	191	275	227	90.4	120	265	105	137	67.9	165
Th	2.9	3.4	0.9	1.9	2.3	2.0	0.9	1.0	1.6	1.5	1.5	0.8	1.1	2.0	0.9	1.5	0.4	1.4
U	0.8	0.9	0.3	0.6	0.6	0.7	0.3	0.3	0.5	0.4	0.4	0.3	0.3	0.5	0.3	0.5	0.1	0.4
Nb	33.6	40.9	13.8	24.9	34.7	23.0	13.9	12.9	18.5	25.3	22.1	13.1	15.9	31.1	13.9	18.5	6.9	17.3
Ta	2.7	3.0	0.8	1.8	2.4	1.6	0.9	0.9	1.3	1.5	1.3	0.7	1.0	1.9	0.8	1.2	0.3	1.1
La	27.8	32.8	11.1	20.8	28.2	20.5	11.8	11.3	17.2	13.6	14.2	8.5	10.2	20.3	11.5	17.1	5.4	15.4
Ce	56.7	65.9	25.6	44.1	59.3	46.0	28.0	26.3	37.8	28.2	29.2	19.7	22.0	42.6	26.2	37.0	12.2	33.4
Pr	6.4	7.4	3.3	5.2	6.9	5.7	3.7	3.5	4.6	3.5	3.5	2.6	2.7	5.2	3.3	4.4	1.5	4.0
Sr	456	457	242	330	487	359	304	343	361	273	233	232	203	384	267	352	412	372
Nd	25.3	29.7	14.6	21.6	28.6	23.7	16.4	15.7	20.4	15.2	14.8	12.2	11.5	22.0	15.1	19.5	7.3	17.8
Sm	4.5	5.4	3.5	4.4	5.6	5.5	4.1	3.9	4.6	3.3	3.0	3.2	2.6	4.5	4.0	4.6	2.0	4.2
Zr	134	147	91.0	120	164	200	131	115	141	86.8	67.3	74.6	63.6	120	106	135	50.3	110
Hf	3.2	3.6	2.4	2.9	3.6	4.6	3.2	2.8	3.4	2.6	2.0	2.2	1.8	3.1	3.0	3.6	1.4	2.9
Eu	1.5	1.7	1.3	1.5	2.0	1.7	1.5	1.4	1.6	1.1	1.0	1.1	0.9	1.6	1.5	1.5	0.9	1.5
Gd	3.9	4.5	3.7	4.1	4.9	5.5	4.7	4.4	4.8	3.0	2.8	3.4	2.4	4.2	4.2	4.4	2.1	4.1
Tb	0.6	0.7	0.6	0.6	0.7	0.8	0.7	0.7	0.7	0.5	0.4	0.6	0.4	0.6	0.7	0.7	0.3	0.7
Dy	3.1	3.5	3.7	3.4	3.9	4.8	4.5	4.1	4.1	2.4	2.2	3.4	2.1	3.3	4.2	3.9	2.0	3.7
Ho	0.6	0.6	0.8	0.7	0.7	0.9	0.9	0.8	0.8	0.4	0.4	0.7	0.4	0.6	0.8	0.7	0.4	0.7
Er	1.5	1.7	2.2	1.9	2.0	2.4	2.4	2.2	2.1	1.1	1.1	1.9	1.2	1.7	2.3	2.0	1.1	2.0
Tm	0.2	0.2	0.3	0.3	0.3	0.4	0.3	0.3	0.3	0.2	0.1	0.3	0.2	0.2	0.3	0.3	0.1	0.3
Yb	1.3	1.4	1.9	1.6	1.8	2.1	2.1	1.8	1.8	1.0	0.9	1.8	1.0	1.5	2.0	1.7	0.9	1.6
Lu	0.2	0.2	0.3	0.2	0.3	0.3	0.3	0.3	0.3	0.1	0.1	0.3	0.1	0.2	0.3	0.2	0.1	0.2
	Olivines									Enrichment percentage (X)								
	JAN 23	JAN 246	SNS 201	SNS 209	SNS 214	HAIN	SAL 690	SAL 768	NAL 759	JAN 23	JAN 246	SNS 201	SNS 209	SNS 214	HAIN	SAL 690	SAL 768	NAL 759
Rb	0.43	0.42	0.05	0.22	0.43	0.19	0.25	0.05	0.20	0.47	0.40	0.75	0.46	0.71	0.57	1.01	0.34	0.77
Ba	7.92	5.87	0.55	3.26	5.41	22.60	3.38	11.20	2.51	0.52	0.43	0.82	0.56	0.77	0.61	1.15	0.57	0.87
Th	0.08	0.07	0.02	0.06	0.09	0.03	0.07	0.02	0.05	0.54	0.47	0.89	0.60	0.87	0.43	1.58	0.41	0.86
U	0.02	0.02	0.00	0.01	0.02	0.01	0.03	0.01	0.01	0.52	0.48	0.87	0.58	0.83	0.41	1.48	0.41	0.86
Nb	1.02	0.85	0.17	0.63	1.10	0.27	0.62	0.16	0.42	0.76	0.55	0.95	0.65	0.90	0.61	1.31	0.54	0.94
Ta	0.06	0.05	0.01	0.03	0.06	0.02	0.03	0.01	0.02	0.58	0.45	0.88	0.56	0.80	0.53	1.27	0.39	0.84
La	0.56	0.55	0.12	0.44	0.64	0.17	0.90	0.14	0.44	0.50	0.44	0.77	0.50	0.73	0.57	1.42	0.48	0.90
Ce	1.11	1.09	0.25	0.97	1.36	0.37	1.62	0.31	0.86	0.51	0.45	0.77	0.51	0.72	0.57	1.30	0.47	0.89
Pr	0.12	0.12	0.03	0.11	0.16	0.05	0.18	0.04	0.10	0.55	0.48	0.81	0.53	0.76	0.58	1.19	0.45	0.87
Sr	6.86	5.21	1.55	5.54	7.70	4.88	25.00	2.19	5.62	0.61	0.52	0.96	0.62	0.79	0.75	1.15	1.20	1.03
Nd	0.48	0.46	0.15	0.44	0.65	0.21	0.72	0.16	0.41	0.61	0.50	0.84	0.54	0.78	0.64	1.18	0.47	0.88
Sm	0.08	0.08	0.03	0.08	0.12	0.05	0.14	0.04	0.08	0.72	0.57	0.91	0.59	0.81	0.74	1.12	0.51	0.92
Zr	3.05	2.44	1.21	2.79	4.51	2.30	5.83	1.57	3.11	0.65	0.47	0.82	0.54	0.74	0.53	1.03	0.44	0.78
Hf	0.07	0.05	0.03	0.06	0.09	0.05	0.12	0.04	0.07	0.81	0.56	0.93	0.62	0.86	0.66	1.13	0.50	0.87
Eu	0.04	0.03	0.01	0.03	0.05	0.08	0.04	0.04	0.03	0.73	0.60	0.90	0.60	0.82	0.89	1.03	0.61	0.95

(*continued on next page*)

Table A1 (*continued*)

	Normal whole-rocks									Olivine enriched whole-rocks								
	JAN 23	JAN 246	SNS 201	SNS 209	SNS 214	HAIN	SAL 690	SAL 768	NAL 759	JAN 23	JAN 246	SNS 201	SNS 209	SNS 214	HAIN	SAL 690	SAL 768	NAL 759
Tb	0.01	0.01	0.01	0.02	0.02	0.01	0.02	0.01	0.01	0.77	0.61	0.90	0.58	0.84	0.76	0.94	0.47	0.86
Gd	0.09	0.09	0.03	0.10	0.14	0.05	0.15	0.04	0.09	0.85	0.69	0.95	0.67	0.90	0.86	0.97	0.52	0.93
Dy	0.08	0.08	0.04	0.09	0.12	0.06	0.14	0.04	0.09	0.78	0.63	0.92	0.63	0.84	0.88	0.87	0.48	0.90
Ho	0.02	0.01	0.01	0.02	0.02	0.02	0.03	0.01	0.02	0.76	0.60	0.87	0.61	0.82	0.89	0.82	0.47	0.88
Er	0.05	0.04	0.04	0.06	0.07	0.07	0.11	0.04	0.07	0.77	0.62	0.88	0.62	0.84	0.95	0.84	0.49	0.94
Tm	0.01	0.01	0.01	0.01	0.01	0.01	0.02	0.01	0.01	0.79	0.61	0.91	0.62	0.88	0.92	0.82	0.49	0.92
Yb	0.04	0.04	0.04	0.05	0.06	0.07	0.10	0.04	0.06	0.78	0.62	0.94	0.64	0.86	0.94	0.81	0.50	0.94
Lu	0.01	0.01	0.01	0.01	0.01	0.01	0.02	0.01	0.01	0.68	0.59	0.92	0.61	0.80	0.94	0.74	0.48	0.84
									Average	0.66	0.54	0.88	0.58	0.81	0.71	1.09	0.51	0.89
									% WR	66.33	53.68	87.65	58.33	81.10	70.58	109.35	50.87	88.75
									% olivine	33.67	46.32	12.35	41.67	18.90	29.42	–	49.13	11.25

Concentrations are in ppm. Assuming that the trace elements concentration differences between the normal and olivine enriched whole-rock powders result from only olivine enrichment, the concentrations C of the "normal WR powder" can be calculated according to the equation: $C_{\text{accumulated rock}} = X \times C_{olivine} + (1 - X) \times C_{wholerock}$ where X is the percentage of artificial olivine enrichment. The average percentage hence obtained is used to correct Os and Re concentrations of olivine-enriched whole-rocks from olivine accumulation.

Table A2
Comparison between olivine corrected whole-rocks and measured whole-rocks values.

	% olivine enrichment	Os (ppb)	Re (ppb)	$^{187}Os/^{188}Os$
JAN23				
WR	33.27	0.12	0.24	0.12431
Olivine		0.08	0.01	0.12446
WR corr		0.14	0.35	0.12423
JAN246				
WR	45.97	0.08	0.13	0.12665
Olivine		0.03	0.03	0.12559
WR corr		0.13	0.22	0.12755
SNS201				
WR	12.29	0.19	0.31	0.13304
Olivine		0.73	0.08	0.13169
WR corr		0.11	0.34	0.13323
SNS209				
WR	41.32	0.19	0.17	0.12738
Olivine		0.10	0.08	0.12743
WR corr		0.25	0.23	0.12735
SNS214				
WR	18.68	0.37	0.23	0.12629
Olivine		0.09	0.04	0.12751
WR corr		0.43	0.27	0.12601
HAIN				
WR	28.46	0.02	0.07	0.13697
Olivine		0.01	0.01	0.13067
WR corr		0.02	0.10	0.13948
SAL690				
WR	0	0.03	0.15	0.13690
Olivine		0.02	0.12	0.13217
WR corr		0.03	0.15	0.13690
SAL768				
WR	50.72	0.07	0.24	0.13237
Olivine		0.01	0.10	0.13431
WR corr		0.12	0.39	0.13038
NAL759				
WR	11.76	0.06	0.59	0.12824
Olivine		0.02	0.04	0.12920
WR corr		0.07	0.66	0.12811

WR for whole-rocks affected by olivine enrichment, WR corr for whole-rocks corrected from olivine enrichment. Percentage of olivine enrichment is from Table A1.

gan Element 2 at Rice University, J. Lupton for access to the helium isotope lab in Newport, OR, which is supported by the NOAA Vents Program. T.S. Johansen, P. Imsland, K. Grønvold, N. Oskarsson, H. Mattsson and F. Holm contributed sample material, information and valuable discussions. The Belgian FRS-FNRS is thanked for present financial support to V.D. M. Thirlwall, J. Lassiter, A. Stracke, B. Hanan, J. Baker, one anonymous reviewer and editor M. Rehkämper are thanked for detailed reviews.

APPENDIX A

See Tables A1–A4.

Table A3
Major element analysis for basalts from Jan Mayen Island and Iceland volcanic flank zones.

	SiO_2	TiO_2	Al_2O_3	FeO	$FeO_{1.5}$	MnO	MgO	CaO	Na_2O	K_2O	P_2O_5	Total
Jan Mayen Island												
JAN23	47.61	2.16	11.46	8.39	1.04	0.16	12.45	13.55	1.74	1.37	0.31	100.23
JAN186	45.37	2.63	14.42	9.39	1.16	0.16	10.47	11.85	2.38	1.22	0.39	99.44
JAN240	47.27	2.10	11.62	8.30	1.02	0.17	11.94	13.32	1.86	1.39	0.34	99.31
JAN246	47.53	2.15	11.53	8.56	1.06	0.17	11.31	13.41	1.79	1.43	0.33	99.25
JAN250	46.61	3.13	15.42	9.74	1.20	0.18	6.58	11.08	2.71	2.40	0.54	99.58
Snæfellness Flank Zone												
SNS201	48.29	1.48	16.00	9.59	1.18	0.18	9.36	11.89	2.21	0.34	0.17	100.67
SNS206	47.01	2.17	15.07	9.35	1.15	0.18	9.10	11.71	2.44	0.50	0.49	99.16
SNS209	46.91	1.74	13.50	9.06	1.12	0.17	12.35	11.47	2.04	0.65	0.28	99.27
SNS211	47.65	1.83	14.68	8.95	1.10	0.19	10.00	10.73	2.67	0.89	0.45	99.12
SNS214	46.04	2.45	14.54	9.71	1.20	0.18	9.95	11.43	2.32	0.88	0.48	99.16
SNS215	45.69	2.34	14.86	9.69	1.20	0.18	9.74	11.86	2.20	0.71	0.48	98.94
SNS219	46.23	2.39	15.08	9.82	1.21	0.18	9.39	11.62	2.22	0.70	0.50	99.33
SNS224	45.63	2.58	14.06	10.29	1.27	0.19	9.97	11.33	2.30	0.76	0.45	98.81
South Flank Zone												
HAIN	46.52	2.01	15.76	9.97	1.23	0.18	9.19	11.06	2.95	0.44	0.26	99.57
STOR	46.16	1.74	14.55	10.15	1.25	0.19	10.55	11.62	2.34	0.21	0.18	98.93
SAL690	49.08	1.83	15.46	8.48	1.05	0.16	7.48	11.42	2.37	0.74	0.22	98.27
SAL690B	47.87	2.16	14.40	9.66	1.19	0.17	8.40	11.40	2.31	0.46	0.26	98.26
Eastern Flank Zone												
SAL761	48.90	2.87	14.09	12.74	1.57	0.23	5.24	9.94	3.23	0.61	0.28	99.69
SAL768	48.77	2.01	16.56	10.01	1.24	0.17	6.57	11.99	2.60	0.41	0.21	100.53
NAL759	48.69	1.96	15.48	9.70	1.20	0.18	8.09	10.87	2.49	0.72	0.27	99.63
NAL780	47.68	1.90	15.04	9.20	1.14	0.16	9.48	11.52	2.24	0.51	0.23	99.08

Values are in wt.%. The precision and accuracy are roughly similar and estimated to 0.6–1.4% for the major element oxides, except Na_2O, K_2O and P_2O_5 (1.8, 7.7 and 5.6%, respectively).

Table A4
Sr isotopic compositions of Iceland picrites corresponding to the samples presented in Brandon et al. (2007).

	$^{87}Sr/^{86}Sr$	2σ
ICE-0	0.703000	±15
ICE-2	0.702895	±11
ICE-3	0.703182	±10
ICE-4a	0.702981	±13
ICE-4b	0.702984	±11
ICE-5	0.703092	±14
ICE-6	0.702925	±14
ICE-8a	0.702967	±8
ICE-8b	0.702964	±10
ICE-9a	0.702949	±13
ICE-10	0.703102	±10
ICE-11	0.703126	±13
DMF-9101	0.703091	±13
9805	0.703052	±8
9806	0.703145	±11
9809	0.703036	±11
9810	0.703151	±15
9812	0.702941	±10
9815	0.703152	±13

See Waight et al. (2002) for detailed analytical techniques.
Errors on isotopic measurements (2σ) are on the two last digits.

REFERENCES

Alard O., Luguet A., Pearson N. J., Griffin W. L., Lorand J. P., Gannoun A., Burton K. W. and O'Reilly S. Y. (2005) In situ Os isotopes in abyssal peridotites bridge the isotopic gap between MORBs and their source mantle. *Nature* **436**, 1005–1008.

Albarède F. (2008) Rogue mantle helium and neon. *Science* **319**, 943–945.

Anders E. and Grevesse N. (1989) Abundances of the elements; meteoritic and solar. *Geochim. Cosmochim. Acta* **53**, 197–214.

Arndt N. T. and Christensen U. (1992) Role of lithospheric mantle in continental volcanism: thermal and geochemical constraints. *J. Geophys. Res.* **97**, 10967–10981.

Becker H. (2000) Re–Os fractionation in eclogites and blueschists and the implications for recycling of oceanic crust into the mantle. *Earth Planet. Sci. Lett.* **177**, 287–300.

Bennett V. C., Norman M. D. and Garcia M. O. (2000) Rhenium and platinum group element abundances correlated with mantle source components in Hawaiian picrites: sulphides in the plume. *Earth Planet. Sci. Lett.* **183**, 513–526.

Bijwaard H. and Spakman W. (1999) Tomographic evidence for a narrow whole mantle plume below Iceland. *Earth Planet. Sci. Lett.* **166**, 121–126.

Birck J.-L., Roy-Barman M. and Capmas F. (1997) Re–Os isotopic measurements at the femtomole level in natural samples. *Geostand. Newslett.* **21**, 19–27.

Bizimis M., Griselin M., Lassiter J. C., Salters V. J. M. and Sen G. (2007) Ancient recycled mantle lithosphere in the Hawaiian plume: osmium–hafnium isotopic evidence from peridotite mantle xenoliths. *Earth Planet. Sci. Lett.* **257**, 259–273.

Blichert-Toft J., Agranier A., Andres M., Kingsley R., Schilling J.-G. and Albarède F. (2005) Geochemical segmentation of the Mid-Atlantic Ridge north of Iceland and ridge-hot spot interaction in the North Atlantic. *Geochem. Geophys. Geosyst.* **6**. doi:10.1029/2004GC000788.

Boyet M. and Carlson R. W. (2005) ^{142}Nd evidence for early (>4.53 Ga) global differentiation of the silicate Earth. *Science* **309**, 576–581.

Boyet M. and Carlson R. W. (2006) A new geochemical model for the Earth's mantle inferred from ^{146}Sm–^{142}Nd systematics. *Earth Planet. Sci. Lett.* **250**, 254–268.

Brandon A. D., Walker R. J. and Puchtel I. S. (2006) Platinum–osmium isotope evolution of the Earth's mantle: constraints from chondrites and Os-rich alloys. *Geochim. Cosmochim. Acta* **70**, 2093–2103.

Brandon A. D., Norman M. D., Walker R. J. and Morgan J. W. (1999) ^{186}Os–^{187}Os systematics of Hawaiian picrites. *Earth Planet. Sci. Lett.* **174**, 25–42.

Brandon A. D., Graham D. W., Waight T. and Gautason B. (2007) ^{186}Os and ^{187}Os enrichments and high-^{3}He/^{4}He sources in the Earth's mantle: evidence from Icelandic picrites. *Geochim. Cosmochim. Acta* **71**, 4570–4591.

Brandon A. D., Snow J. E., Walker R. J., Morgan J. W. and Mock T. D. (2000) Pt-190-Os-186 and Re-187-Os-187 systematics of abyssal peridotites. *Earth Planet. Sci. Lett.* **177**, 319–335.

Breddam K. (2002) Kistufell: primitive melt from the Iceland mantle plume. *J. Petrol.* **43**, 345–373.

Breddam K., Kurz M. D. and Storey M. (2000) Mapping out the conduit of the Iceland mantle plume with helium isotopes. *Earth Planet. Sci. Lett.* **176**, 45–55.

Breivik A. J., Mjelde R., Faleide J. I. and Murai Y. (2006) Rates of continental breakup magmatism and seafloor spreading in the Norway Basin–Iceland plume interaction. *J. Geophys. Res.* **111**, B07102. doi:10.1029/2005JB004004.

Chauvel C. and Hémond C. (2000) Melting of a complete section of oceanic crust: trace element and Pb isotopic evidence from Iceland. *Geochem. Geophys. Geosyst.* **1**, doi:10.1029/1999GC000002.

Chauvel C., Hofmann A. W. and Vidal P. (1992) HIMU-EM: the French Polynesian connection. *Earth Planet. Sci. Lett.* **110**, 99–119.

Class C. and Goldstein S. L. (1997) Plume–lithosphere interactions in the ocean basins: constraints from the source mineralogy. *Earth Planet. Sci. Lett.* **150**, 245–260.

Class C. and Goldstein S. L. (2005) Evolution of helium isotopes in the Earth's mantle. *Nature* **436**, 1107–1112.

Cohen A. S. and Waters F. G. (1996) Separation of osmium from geological materials by solvent extraction for analysis by thermal ionisation mass spectrometry. *Anal. Chim. Acta* **332**, 269–275.

Coltice N. and Ricard Y. (1999) Geochemical observations and one layer mantle convection. *Earth Planet. Sci. Lett.* **174**, 125–137.

Condomines M., Grönvold K., Hooker P. J., Muehlenbachs K., O'Nions R. K., Oskarsson N. and Oxburgh E. R. (1983) Helium, oxygen, strontium and neodymium isotopic relationships in Iceland volcanics. *Earth Planet. Sci. Lett.* **66**, 125–136.

Dallmann W. K., Ohta Y., Elvevold S. and Blomeier D. (eds.) (2002) Bedrock map of Svalbard and Jan Mayen, 1:750000. In: *Norsk Polarinstitutt*.

Debaille V., Doucelance R., Weis D. and Schiano P. (2006a) Multi-stage mixing in subduction zones: application to Merapi volcano (Java island, Sunda arc). *Geochim. Cosmochim. Acta* **70**, 723–741.

Debaille V., Blichert-Toft J., Agranier A., Doucelance R., Schiano P. and Albarède F. (2006b) Geochemical component relationships in MORB from the Mid-Atlantic Ridge, 22–35°N. *Earth Planet. Sci. Lett.* **241**, 844–862.

Dixon E. T. (2003) Interpretation of helium and neon isotopic heterogeneity in Icelandic basalts. *Earth Planet. Sci. Lett.* **206**, 83–99.

Dixon E. T., Honda M., McDougall I., Campbell I. H. and Sigurdsson I. (2000) Preservation of near-solar neon isotopic ratios in Icelandic basalts. *Earth Planet. Sci. Lett.* **180**, 309–324.

Douglass J. and Schilling J.-G. (2000) Systematics of three-component, pseudo-binary mixing lines in 2D isotope ratio space representations and implications for mantle plume–ridge interaction. *Chem. Geol.* **163**, 1–23.

Eisele J., Sharma M., Galer S. G., Blichert-Toft J., Devey C. W. and Hofmann A. W. (2002) The role of sediment recycling in EM-1 inferred from Os, Pb, Hf, Nd, Sr isotope and trace element systematics of the Pitcairn hotspot. *Earth Planet. Sci. Lett.* **196**, 197–212.

Ellam R. M. and Stuart F. M. (2004) Coherent He–Nd–Sr isotope trends in high ^{3}He/^{4}He basalts: implications for a common reservoir, mantle heterogeneity and convection. *Earth Planet. Sci. Lett.* **228**, 511–523.

Ellam R. M., Carlson R. W. and Shirey S. B. (1992) Evidence from Re–Os isotopes for plume–lithosphere mixing in Karoo flood basalt genesis. *Nature* **359**, 718–721.

Elliott T. R., Hawkesworth C. J. and Gronvold K. (1991) Dynamic melting of the Iceland plume. *Nature* **351**, 201–206.

Farley K. A. and Neroda E. (1998) Noble gases in the Earth's mantle. *Annu. Rev. Earth Planet. Sci.* **26**, 189–218.

Fitton J. G., Saunders A., Kempton P. D. and Hardarson B. S. (2003) Does depleted mantle form an intrinsic part of the Iceland plume? *Geochem. Geophys. Geosyst.* **4**. doi:10.1029/2002GC000424.

Fitton J. G., Saunders A. D., Norry M. J., Hardarson B. S. and Taylor R. N. (1997) Thermal and chemical structure of the Iceland plume. *Earth Planet. Sci. Lett.* **153**, 197–208.

Foulger G. R., Natland J. H. and Anderson D. (2005) A source for Icelandic magmas in remelted Iapetus crust. *J. Volcanol. Geotherm. Res.* **141**, 23–44.

Foulger G. R., Pritchard M. J., Julian B. R., Evans J. R., Allen R. M., Nolet G., Morgan W. J., Bergsson B. H., Erlendsson P., Jakobsdottir S., Ragnarsson S., Stefansson R. and Vogfjord K. (2001) Seismic tomography shows that upwelling beneath Iceland is confined to the upper mantle. *Geophys. J. Int.* **146**, 504–530.

Furman T., Frey F. A. and Park K.-H. (1991) Chemical constraints on the petrogenesis of mildly alkaline lavas from Vestmannaeyjar, Iceland: the Eldfell (1973) and Surtsey (1963–1967) eruptions. *Contrib. Mineral. Petrol.* **109**, 19–37.

Gannoun A., Burton K. W., Parkinson I. J., Alard O., Schiano P. and Thomas L. E. (2007) The scale and origin of the osmium isotope variations in mid-ocean ridge basalts. *Earth Planet. Sci. Lett.* **259**, 541–556.

Gautheron C. and Moreira M. (2002) Helium signature of the subcontinental lithospheric mantle. *Earth Planet. Sci. Lett.* **199**, 39–47.

Gee M. A. M., Thirlwall M. F., Taylor R. N., Lowry D. and Murton B. J. (1998) Crustal processes: major controls on Reykjanes Peninsula lava chemistry, SW Iceland. *J. Petrol.* **39**, 819–839.

Georgen J. E. and Lin J. (2003) Plume-transform interactions at ultra-slow spreading ridges: implications for the Southwest Indian Ridge. *Geochem. Geophys. Geosyst.* **4**. doi:10.1029/2003GC000542.

Goldstein S. L., Soffer G., Langmuir C. H., Lehnert K. A., Graham D. W. and Michael P. J. (2008) Origin of a "Southern Hemisphere" geochemical signature in the Arctic upper mantle. *Nature* **453**, 89–93.

Graham D., Larsen L. M., Hanan B. B., Storey M., Pedersen A. K. and Lupton J. E. (1998) Helium isotope composition of the early Iceland mantle plume inferred from Tertiary picrites of West Greenland. *Earth Planet. Sci. Lett.* **160**, 241–255.

Graham D. W. (2002) Noble gas isotope geochemistry of mid-ocean ridge and ocean island basalts: characterization of mantle source reservoirs. In *Noble Gases in Geochemistry and Cosmo-*

chemistry. Reviews in Mineralogy and Geochemistry (eds. D. Porcelli, R. Wieler and R. Ballentine). Mineral. Soc. Amer., Washington, DC, pp. 247–318.

Haase K. M., Devey C. W., Mertz D. F., Stoffers P. and Garbe-Schonberg D. (1996) Geochemistry of lavas from Mohns Ridge, Norwegian–Greenland Sea: implications for melting conditions and magma sources near Jan Mayen. *Contrib. Mineral. Petrol.* **123**, 223–237.

Hanan B. B. and Schilling J.-G. (1986) Source origin of Iceland Basalt volcanism: Pb isotopes in the Eastern Iceland Tertiary section. *Terra Cognita* **6**, 189.

Hanan B. B. and Graham D. W. (1996) Lead and helium isotope evidence from oceanic basalts for a common deep source of mantle plumes. *Science* **272**, 991–995.

Hanan B. B. and Schilling J.-G. (1997) The dynamic evolution of the Iceland mantle plume: the lead isotope perspective. *Earth Planet. Sci. Lett.* **151**, 43–60.

Hanan B. B., Kingsley R. H. and Schilling J.-G. (1986) Pb isotope evidence in the South Atlantic for migrating ridge–hotspot interactions. *Nature* **322**, 137–144.

Hanan B. B., Blichert-Toft J., Kingsley R. and Schilling J.-G. (2000) Depleted Iceland mantle plume geochemical signature: artifact of multicomponent mixing? *Geochem. Geophys. Geosyst.* **1**, doi:10.1029/1999GC000009.

Hanyu T. and Kaneoka I. (1997) The uniform and low $^{3}He/^{4}He$ ratios of HIMU basalts as evidence for as recycled materials. *Nature* **390**, 273–276.

Hards V. L., Kempton P. D. and Thompson R. N. (1995) The heterogeneous Iceland plume – new insights from the alkaline basalts of the Snaefell volcanic center. *J. Geol. Soc.* **152**, 1003–1009.

Hards V. L., Kempton P. D., Thompson R. N. and Greenwood P. B. (2000) The magmatic evolution of the Snaefell volcanic centre; an example of volcanism during incipient rifting in Iceland. *J. Volcanol. Geotherm. Res.* **99**, 97–121.

Harvey J., Gannoun A., Burton K. W., Rogers N. W., Alard O. and Parkinson I. J. (2006) Ancient melt extraction from the oceanic upper mantle revealed by Re–Os isotopes in abyssal peridotites from the Mid-Atlantic ridge. *Earth Planet. Sci. Lett.* **244**, 606–621.

Hassler D. R. and Shimizu N. (1998) Osmium isotopic evidence for ancient subcontinental lithospheric mantle beneath the Kerguelen Islands, Southern Indian Ocean. *Science* **280**, 418–421.

Hauri E. H. and Hart S. R. (1993) Re–Os isotope systematics of HIMU and EMII oceanic island basalts from the south Pacific Ocean. *Earth Planet. Sci. Lett.* **114**, 353–371.

Hauri E. H. and Hart S. R. (1997) Rhenium abundances and systematics in oceanic basalts. *Chem. Geol.* **139**, 185–205.

Hauri E. H., Whitehead J. A. and Hart S. R. (1994) Fluid dynamic and geochemical aspects of entrainment in mantle plumes. *J. Geophys. Res.* **99**, 24275–24300.

Havskov J. and Atakan K. (1991) Seismicity and volcanism of Jan Mayen Island. *Terra Nova* **3**, 517–526.

Helmberger D. V., Wen L. and Ding X. (1998) Seismic evidence that the source of the Iceland hotspot lies at the core–mantle boundary. *Nature* **396**, 251–255.

Hémond C., Arndt N. T., Lichtenstein U. and Hofmann A. W. (1993) The heterogeneous Iceland plume: Nd–Sr–O isotopes and trace element constraints. *J. Geophys. Res.* **98**, 15833–15850.

Ingle S., Weis D. and Frey F. A. (2002) Indian continental crust recovered from Elan Bank, Kerguelen Plateau (ODP Leg 183, Site 113). *J. Petrol.* **43**, 1241–1257.

Ito G. (2001) Reykjanes 'V'-shaped ridges originating from a pulsing and dehydrating mantle plume. *Nature* **411**, 681–684.

Jackson M. G., Hart S. R., Saal A. E., Shimizu N., Kurz M. D., Blusztajn J. S. and Skovgaard A. C. (2008) Globally elevated titanium, tantalum, and niobium (TITAN) in ocean island basalts with high $^{3}He/^{4}He$. *Geochem. Geophys. Geosyst.* **9**. doi:10.1029/2007GC001876.

Jones S. M., White N. and Maclennan J. (2002) V-shaped ridges around Iceland: implications for spatial and temporal patterns of mantle convection. *Geochem. Geophys. Geosyst.* **3**, 1059. doi:10.1029/2002GC000361.

Jordan T. H. (1988) Structure and formation of the continental tectosphere. *J. Petrol. Special Lithosphere Issue*, 11–37.

Kempton P. D., Fitton J. G., Saunders A. D., Nowell G. M., Taylor R. N., Hardarson B. S. and Pearson D. G. (2000) The Iceland plume in space and time: a Sr–Nd–Pb–Hf study of the North Atlantic rifted margin. *Earth Planet. Sci. Lett.* **177**, 255–271.

Kerr A. C. (1995) The melting process and the composition of the North Atlantic mantle–plume: geochemical evidence form the Early Tertiary basalts. *J. Geol. Soc. Lond.* **152**, 975–978.

Kerr A. C., Saunders A. D., Tarney J., Berry N. H. and Hards V. L. (1995) Depleted mantle–plume geochemical signatures: no paradox for plume theories. *Geology* **23**, 843–846.

Kokfelt T. F., Hoernle K., Hauff F., Fiebig J., Werner R. and Garbe-Schonberg D. (2006) Combined trace element and Pb–Nd–Sr–O isotope evidence for recycled oceanic crust (upper and lower) in the Iceland mantle plume. *J. Petrol.* **47**, 1705–1749.

Kristjansson L., Johannesson H., Eiriksson J. and Gudmundsson A. I. (1988) Bruhnes-Matuyama paleomagnetism in three lava sections in Iceland. *Can. J. Earth Sci.* **25**, 215–225.

Kurz M. D., Jenkins W. J., Schilling J.-G. and Hart S. R. (1982) Helium isotopic variation in the mantle beneath the central North Atlantic Ocean. *Earth Planet. Sci. Lett.* **58**, 1–14.

Larsen L. M., Pedersen A. K., Sundvoll B. and Frei R. (2003) Alkali picrites formed by melting of old metasomatised lithospheric mantle: Manitdlat member, Vaigat formation, Paleocene of West Greenland. *J. Petrol.* **44**, 3–38.

Lassiter J. C. (2003) Rhenium volatility in subaerial lavas: constraints from subaerial and submarine portions of the HSDP-2 Mauna Kea drillcore. *Earth Planet. Sci. Lett.* **214**, 311–325.

Lassiter J. C. and Hauri E. H. (1998) Osmium-isotope variations in Hawaiian lavas: evidence for recycled oceanic lithosphere in the Hawaiian plume. *Earth Planet. Sci. Lett.* **164**, 483–496.

Lee C.-T. A. (2002) Platinum-group element geochemistry of peridotite xenoliths from the Sierra Nevada and the Basin and Range, California. *Geochim. Cosmochim. Acta* **66**, 3987–4005.

Lee D.-C., Halliday A. N., Fitton J. G. and Poli G. (1994) Isotopic variations with distance and time in the volcanic islands of the Cameroon Line-evidence for a mantle plume origin. *Earth Planet. Sci. Lett.* **123**, 119–138.

Lee S. R. and Walker R. J. (2006) Re–Os isotope systematics of mantle xenoliths from South Korea: evidence for complex growth and loss of lithospheric mantle beneath East Asia. *Chem. Geol.* **231**, 90–101.

Levasseur S., Birck J. L. and Allègre C. J. (1998) Direct measurement of femtomoles of osmium and the $^{187}Os/^{186}Os$ in sea water. *Science* **282**, 272–274.

Li X., Kind R. and Yuan X. (2003) Seismic study of upper mantle and transition zone beneath hotspots. *Phys. Earth Planet. Interiors* **136**, 79–92.

Liu C. Z., Snow J. E., Hellebrand E., Brugmann G., von der Handt A., Buchl A. and Hofmann A. W. (2008) Ancient, highly heterogeneous mantle beneath Gakkel ridge, Arctic Ocean. *Nature* **452**, 311–316.

Luais B., Telouk P. and Albarède F. (1997) Precise and accurate neodymium isotopic measurements by plasma-source mass spectrometry. *Geochim. Cosmochim. Acta* **61**, 4847–4854.

Luck J. M. and Allègre C. (1983) ^{187}Re–^{187}Os systematics in meteorites and cosmochemical consequences. *Nature* **302**, 130–132.

Macdonald R., Sparks R. S. J., Sigurdsson H., Mattey D. P., Mcgarvie D. W. and Smith R. L. (1987) The 1875 eruption of Askja Volcano, Iceland: combined fractional crystallization and selective contamination in the generation of rhyolithic magma. *Mineral. Mag.* **51**, 183–202.

Macpherson C. G., Hilton D. R., Day J. M. D., Lowry D. and Gronvold K. (2005) High-^{3}He/^{4}He, depleted mantle and low-δ^{18}O, recycled oceanic lithosphere in the source of central Iceland magmatism. *Earth Planet. Sci. Lett.* **233**, 411–427.

Mahoney J., Nicollet C. and Dupuy C. (1991) Madagascar basalts: tracking oceanic and continental sources. *Earth Planet. Sci. Lett.* **104**, 350–363.

Martin C. E. (1991) Os isotopic characteristics of mantle derived rocks. *Geochim. Cosmochim. Acta* **55**, 1421–1434.

Martin C. E., Carlson R. W., Shirey S. B., Frey F. A. and Chen C.-Y. (1994) Os isotopic variation in basalts from Haleakala Volcano, Maui, Hawaii: a record of magmatic processes in oceanic mantle and crust. *Earth Planet. Sci. Lett.* **128**, 287–301.

Mattson H. and Höskuldsson A. (2003) Geology of the Heimaey volcanic center, south Iceland: early evolution of a central volcano in a propagating rift? *J. Volcanol. Geotherm. Res.* **127**, 55–71.

McDonough W. F. (1990) Constraints on the composition of the continental lithospheric mantle. *Earth Planet. Sci. Lett.* **101**, 1–18.

McDonough W. F. and Sun S. S. (1995) Composition of the Earth. *Chem. Geol.* **120**, 223–253.

McKenzie D. and O'Nions R. K. (1983) Mantle reservoirs and oceanic island basalts. *Nature* **301**, 229–231.

Meisel T., Walker R. J., Irving A. J. and Lorand J.-P. (2001) Osmium isotopic compositions of mantle xenoliths: a global perspective. *Geochim. Cosmochim. Acta* **65**, 1311–1323.

Menke W., Brandsdottir B. and Einarsson P. (1996) Reinterpretation of the RRISP-77 Iceland shear-wave profiles. *Geophys. J. Int.* **126**, 166–172.

Mertz D. F., Sharp W. D. and Haase K. M. (2004) Volcanism on the Eggvin Bank (Central Norwegian–Greenland Sea, latitude 71°N): age, source, and relationship to the Iceland and putative Jan Mayen plumes. *J. Geodyn.* **38**, 57–83.

Mertz D. F., Devey C. W., Todt W., Stoffers P. and Hofmann A. W. (1991) Sr–Nd–Pb isotope evidence against plume–asthenosphere mixing north of Iceland. *Earth Planet. Sci. Lett.* **107**, 243–255.

Milner S. C. and LeRoex A. P. (1996) Isotope characteristics of the Okenyenya igneous complex, northwestern Namibia: constraints on the composition of the early Tristan plume and the origin of the EM1 mantle component. *Earth Planet. Sci. Lett.* **141**, 277–291.

Montelli R., Nolet G., Dahlen F. A. and Masters G. (2006) A catalogue of deep mantle plumes: new results from finite-frequency tomography. *Geochem. Geophys. Geosyst.* **7**. doi:10.1029/2006GC001248.

Montelli R., Nolet G., Dahlen F. A., Masters G., Engdahl E. R. and Hung S. H. (2004) Finite-frequency tomography reveals a variety of plumes in the mantle. *Science* **303**, 338–343.

Moreira M. and Kurz M. D. (2001) Subducted oceanic lithosphere and the origin of the "high μ" basalt helium isotopic signature. *Earth Planet. Sci. Lett.* **189**, 49–57.

Moreira M., Breddam K., Curtice J. and Kurz M. D. (2001) Solar neon in the Icelandic mantle: new evidence for an undegassed lower mantle. *Earth Planet. Sci. Lett.* **185**, 15–23.

Morgan J. W. (1986) Ultramafic xenoliths: clues to Earth's late accretionary history. *J. Geophys. Res.* **91**, 12375–12387.

Mosar J., Eide E., Osmundsen P. T., Sommaruga A. and Torsvik T. H. (2002) Greenland–Norway separation: a geodynamic model for the North Atlantic. *Norw. J. Geol.* **82**, 281–298.

Neal C. R. (2001) Interior of the Moon: the presence of garnet in the primitive deep lunar mantle. *J. Geophys. Res.* **106**, 27865–27885.

Nicholson H., Condomines M., Fitton j. G., Fallick A. E., Grönvold K. and Rogers G. (1991) Geochemical and isotopic evidence for crustal assimilation beneath Krafla, Iceland. *J. Petrol.* **32**, 1005–1020.

Niu Y. L. and O'Hara M. J. (2003) Origin of ocean island basalts: a new perspective from petrology, geochemistry, and mineral physics considerations. *J. Geophys. Res.* **108**, 2209. doi:10.1029/2002JB002048.

Parman S. W., Kurz M. D., Hart S. R. and Grove T. L. (2005) Helium solubility in olivine and implications for high ^{3}He/^{4}He in ocean island basalts. *Nature* **437**, 1140–1143.

Pearson D. G., Carlson R. W., Shirey S. B., Boyd F. R. and Nixon P. H. (1995) Stabilisation of Archean lithospheric mantle: a Re–Os isotope study of peridotite xenoliths from the Kaapvaal craton. *Earth Planet. Sci. Lett.* **134**, 341–357.

Peucker-Ehrenbrink B. and Jahn B.-M. (2001) Rhenium–osmium isotope systematics and platinum group element concentrations: loess and the upper continental crust. *Geochem. Geophys. Geosyst.* **2**. doi:10.1029/2001GC000172.

Porcelli D. and Elliot T. (2008) The evolution of He Isotopes in the convecting mantle and the preservation of high ^{3}He/^{4}He ratios. *Earth Planet. Sci. Lett.* **269**, 175–185.

Poreda R., Schilling J.-G. and Craig H. (1986) Helium and hydrogen isotope in ocean-ridge basalts north and south of Iceland. *Earth Planet. Sci. Lett.* **78**, 1–17.

Prestvik T., Goldberg S., Karlsson H. and Gronvold K. (2001) Anomalous strontium and lead isotope signatures in the off-rift Öræfajökull central volcano in south-east Iceland. Evidence for enriched endmember(s) of the Iceland mantle plume? *Earth Planet. Sci. Lett.* **190**, 211–220.

Rehkämper M. and Hofmann A. W. (1997) Recycled ocean crust and sediment in Indian Ocean MORB. *Earth Planet. Sci. Lett.* **147**, 93–106.

Reisberg L., Zindler A., Marcantonio F., White W., Wyman D. and Weaver B. (1993) Os systematics in ocean island basalts. *Earth Planet. Sci. Lett.* **120**, 149–167.

Reisberg L. C., Allègre C. J. and Luck J.-M. (1991) The Re–Os systematics of the Ronda ultramafic complex of southern Spain. *Earth Planet. Sci. Lett.* **105**, 196–213.

Roy-Barman M. and Allègre C. J. (1994) ^{187}Os/^{186}Os ratios of mid-ocean ridge basalts and abyssal peridotites. *Geochim. Cosmochim. Acta* **58**, 5043–5054.

Roy-Barman M. and Allègre C. J. (1995) ^{187}Os/^{186}Os in oceanic island basalts: tracing oceanic crust recycling in the mantle. *Earth Planet. Sci. Lett.* **129**, 145–161.

Sæmundsson K. (1979) Outline of the geology of Iceland. *Jokull* **29**, 7–28.

Schaefer B. F., Turner S., Parkinson I. J., Rogers N. W. and Hawkesworth C. J. (2002) Evidence for recycled Archaean oceanic mantle lithosphere in the Azores plume. *Nature* **420**, 304–307.

Schiano P., Burton K. W., Dupre B., Birck J.-L., Guille G. and Allègre C. J. (2001) Correlated Os–Pb–Nd–Sr isotopes in the Austral-Cook chain basalts: the nature of mantle components in plume sources. *Earth Planet. Sci. Lett.* **186**, 527–537.

Schilling J.-G. (1973) Iceland mantle plume: geochemical study of Reykjanes Ridge. *Nature* **242**, 565–571.

Schilling J.-G. and Noe-Nygaard A. (1974) Faeroe-Iceland plume: rare earth evidence. *Earth Planet. Sci. Lett.* **24**, 1–14.

Schilling J.-G., Kingsley R. H., Hanan B. B. and McCully B. L. (1992) Nd–Sr–Pb isotopic variations along the Gulf of Aden: evidence for Afar mantle plume–continental lithosphere interaction. *J. Geophys. Res.* **97**, 10927–10966.

Schilling J.-G., Kingsley R., Fontignie D., Poreda R. and Xue S. (1999) Dispersion of the Jan Mayen and Iceland mantle plumes in the Arctic: a He–Pb–Nd–Sr isotope tracer study of basalts from the Kolbeinsey, Mohns and Knipovitch ridges. *J. Geophys. Res.* **104**, 10543–10569.

Schilling J.-G., Zajac M., Evans R., Johnston T., White W., Devine J. D. and Kingsley R. (1983) Petrologic and geochemical variations along the Mid-Atlantic Ridge from 29°N to 73°N. *Am. J. Sci.* **283**, 510–586.

Shen Y., Solomon S., Bjarnason I. and Nolet G. (2002) Seismic evidence for a tilted mantle plume and north–south mantle flow beneath Iceland. *Earth Planet. Sci. Lett.* **197**, 261–272.

Shirey S. B. and Walker R. J. (1995) Carius tube digestions for low-blank rhenium–osmium analysis. *Anal. Chem.* **67**, 2136–2141.

Shirey S. B. and Walker R. J. (1998) The Re–Os isotope system in cosmochemistry and high-temperature geochemistry. *Ann. Rev. Earth Planet. Sci.* **26**, 423–500.

Sigmarsson O. (1996) Short magma chamber residence time at an Icelandic volcano inferred from U-series disequilibria. *Nature* **382**, 440–442.

Sigmarsson O., Condomines M. and Fourcade S. (1992) Mantle and crustal contribution in the genesis of recent basalts from off-rift zones in Iceland: constraints from Th, Sr, and O isotopes. *Earth Planet. Sci. Lett.* **110**, 149–162.

Sigmarsson O., Karlsson H. R. and Larsen G. (2000) The 1996 and 1998 subglacial eruptions beneath the Vatnajokull ice sheet in Iceland: contrasting geochemical and geophysical inferences on magma migration. *Bull. Volc.* **61**, 468–476.

Sigmarsson O., Hemond C., Condomines M., Fourcade S. and Oskarsson N. (1991) Origin of silicic magma in Iceland revealed by Th isotopes. *Geology* **19**, 621–624.

Skovgaard A. C., Storey M., Baker J., Blusztajn J. and Hart S. R. (2001) Osmium–oxygen isotopic evidence for a recycled and strongly depleted component in the Iceland mantle plume. *Earth Planet. Sci. Lett.* **194**, 259–275.

Snow J. E. and Reisberg L. (1995) Os isotopic systematics of the MORB mantle: results from altered abyssal peridotites. *Earth Planet. Sci. Lett.* **133**, 411–421.

Snow J. E., Hart S. R. and Dick H. J. B. (1994) Nd and Sr isotope evidence linking mid-ocean-ridge basalts and abyssal peridotites. *Nature* **371**, 57–60.

Sobolev A. V., Hofmann A. W., Kuzmin D. V., Yaxley G. M., Arndt N. T., Chung S. L., Danyushevsky L. V., Elliott T., Frey F. A., Garcia M. O., Gurenko A. A., Kamenetsky V. S., Kerr A. C., Krivolutskaya N. A., Matvienkov V. V., Nikogosian I. K., Rocholl A., Sigurdsson I. A., Sushchevskaya N. M. and Teklay M. (2007) The amount of recycled crust in sources of mantle-derived melts. *Science* **316**, 412–417.

Staples R. K., White R. S., Brandsdottir B., Menke W., Maguire P. K. H. and McBride J. H. (1997) Faroe-Iceland ridge experiment 1. Crustal structure of northeastern Iceland. *J. Geophys. Res.* **102**, 7849–7866.

Steinthorsson S., Hardarson B. S., Ellam R. M. and Larsen G. (2000) Petrochemistry of the Gjalp-1996 subglacial eruption, Vatnajökull, SE Iceland. *J. Volcanol. Geotherm. Res.* **98**, 79–90.

Stracke A., Bizimis M. and Salters V. J. M. (2003) Recycling oceanic crust: quantitative constraints. *Geochem. Geophys. Geosyst.* **4**. doi:10.1029/2002GC000347.

Stracke A., Zindler A., Blichert-Toft J., Albarède F. and McKenzie D. (1998) Hafnium and strontium isotope measurements in high-MgO basalts from Theistareykir, northern Iceland. *Mineral. Mag.* **62A**, 1464–1465.

Stuart F. M., Lass-Evans S., Fitton J. G. and Ellam R. M. (2003) High He-3/He-4 ratios in picritic basalts from Baffin Island and the role of a mixed reservoir in mantle plumes. *Nature* **424**, 57–59.

Sun W., Bennett V. C. and Kamenetsky V. S. (2004) The mechanism of Re enrichment in arc magmas: evidence from Lau Basin basaltic glasses and primitive melt inclusions. *Earth Planet. Sci. Lett.* **222**, 101–114.

Sun W., Bennett V. C., Eggins S. M., Kamenetsky V. S. and Arculus R. J. (2003) Enhanced mantle-to-crust rhenium transfer in undegassed arc magmas. *Nature* **422**, 294–297.

Thirlwall M. F. (1995) Generation of the Pb isotopic characteristics of the Iceland plume. *J. Geol. Soc.* **152**, 991–996.

Thirlwall M. F. (1997) Pb isotopic and elemental evidence for OIB derivation from young HIMU mantle. *Chem. Geol.* **139**, 51–74.

Thirlwall M. F., Gee M. A. M., Taylor R. N. and Murton B. J. (2004) Mantle components in Iceland and adjacent ridges investigated using double-spike Pb isotope ratios. *Geochim. Cosmochim. Acta* **68**, 361–386.

Thirlwall M. F., Gee M. A. M., Lowry D., Mattey D. P., Murton B. J. and Taylor R. N. (2006) Low delta O-18 in the Icelandic mantle and its origins: evidence from Reyjanes Ridge and Icelandic lavas. *Geochim. Cosmochim. Acta* **70**, 993–1019.

Trønnes R. G., Planke S., Sundvoll B. and Imsland P. (1999) Recent volcanic rocks from Jan Mayen: low-degree melt fractions of enriched northeast Atlantic mantle. *J. Geophys. Res.* **104**, 7153–7168.

Waight T., Baker J. and Peate D. (2002) Sr isotope ratio measurements by double-focusing MC-ICPMS: techniques, observations and pitfalls. *Int. J. Mass Spec.* **221**, 229–244.

Walker R. J. and Morgan J. W. (1989) Rhenium–osmium isotope systematics of carbonaceous chondrites. *Science* **243**, 519–522.

Walker R. J., Carlson R. W., Shirey S. B. and Boyd F. R. (1989) Os, Sr, Nd and Pb isotope systematics of southern African peridotite xenoliths: implications for the chemical evolution of subcontinental mantle. *Geochim. Cosmochim. Acta* **53**, 1583–1595.

Weaver B. L. (1991) The origin of ocean island basalt end-member compositions: trace element and isotopic constraints. *Earth Planet. Sci. Lett.* **104**, 381–397.

White W. M., McBirney A. R. and Duncan B. (1993) Petrology and geochemistry of Galapagos: portrait of a pathological mantle plume. *J. Geophys. Res.* **93**, 19533–19563.

Widom E. and Shirey S. B. (1996) Os isotope systematics in the Azores: implications for mantle plume sources. *Earth Planet. Sci. Lett.* **142**, 451–465.

Widom E., Hoernle K. A., Shirey S. B. and Schminke H.-U. (1999) Os isotope systematics in the Canary Islands and Madeira: lithospheric contamination and mantle plume signatures. *J. Petrol.* **40**, 279–296.

Workman R. K. and Hart S. R. (2005) Major and trace element composition of the depleted MORB mantle (DMM). *Earth Planet. Sci. Lett.* **231**, 53–72.

Zhao D. (2004) Global tomographic images of mantle plumes and subducting slabs: insight into deep Earth dynamics. *Phys. Earth Planet. Interiors* **146**, 3–34.

Zindler A. and Hart S. (1986) Chemical geodynamics. *Ann. Rev. Earth Planet. Sci.* **14**, 493–571.

Zindler A., Hart S. R., Frey F. A. and Jakobsson S. (1979) Nd and Sr isotope ratios and rare earth element abundances in Reykjanes peninsula basalts: evidence for mantle heterogeneity beneath Iceland. *Earth Planet. Sci. Lett.* **45**, 249–262.

Associate editor: Mark Rehkämper